

SURFACE AREA STUDIES OF HIGH VACUUM

EVAPORATED NICKEL FILMS

THESIS SUBMITTED FOR THE DEGREE OF

DOCTOR OF PHILOSOPHY

OF THE UNIVERSITY OF GLASGOW

By

DAVID T. DUTHIE

OCTOBER, 1963

ProQuest Number: 13849482

All rights reserved

INFORMATION TO ALL USERS

The quality of this reproduction is dependent upon the quality of the copy submitted.

In the unlikely event that the author did not send a complete manuscript and there are missing pages, these will be noted. Also, if material had to be removed, a note will indicate the deletion.



ProQuest 13849482

Published by ProQuest LLC (2019). Copyright of the Dissertation is held by the Author.

All rights reserved.

This work is protected against unauthorized copying under Title 17, United States Code  
Microform Edition © ProQuest LLC.

ProQuest LLC.  
789 East Eisenhower Parkway  
P.O. Box 1346  
Ann Arbor, MI 48106 – 1346

## ACKNOWLEDGMENTS

The author wishes to express his sincere thanks to his supervisor, Dr. K. C. Campbell, for his encouragement and guidance.

The author also wishes to thank Dr. S. J. Thomson and Dr. I. Hoodless for many helpful and stimulating discussions, and Mr. J. McAllister for the analysis of the nickel films.

This research was supported by a grant from the Department of Scientific and Industrial Research.

1.1	Introduction	35
1.2	The Surface Dipole Mechanism	39
1.3	The Electron Transfer Mechanism	57
1.4	Results and Discussion of Hydrogen Absorption Experiments	61
1.5	Results and Discussion of Hydrogen and Oxygen Coverage	67

## CONTENTS

	<u>Page No.</u>
<u>INTRODUCTION</u> .....	1
<u>CHAPTER 1 - THEORETICAL BASIS OF EXPERIMENTAL METHOD</u>	
1.1. Introduction .....	10
1.2. Measurement of Surface Areas .....	12
1.3. One Point Methods .....	18
1.4. Independent One Point Method .....	21
1.5. Thermal Transpiration .....	23
<u>CHAPTER 2 - SURFACE AREA MEASUREMENTS ON OXYGEN AND NITROUS OXIDE OXYGENATED FILMS</u>	
2.1. Apparatus .....	27
2.2. Results of Oxygen and Nitrous Oxide Oxygenated Films ..	28
2.3. Discussion of Results of Oxygenated Films .....	30
2.4. Results and Discussion of Films which have been Oxygenated by both Oxygen and Nitrous Oxide .....	36
2.5. General Discussion .....	37
<u>CHAPTER 3 - THE ADSORPTION OF KRYPTON <del>By</del> NICKEL FILMS ON WHICH HYDROGEN AND OXYGEN HAS BEEN CHEMISORBED, AND ON WHICH ETHYLENE AND OXYGEN HAS BEEN CHEMISORBED</u>	
3.1. Introduction .....	42
3.2. The Surface Dipole Mechanism .....	44
3.3. The Electron Transfer Mechanism .....	51
3.4. Results and Discussion of Hydrogen Adsorption Experiments .....	52
3.5. Results and Discussion of Hydrogen and Oxygen Covered Films .....	56

3.6.	Results and Discussion of Films which have Adsorbed Ethylene .....	57
3.7.	Results and Discussion of Krypton Adsorption Measurements on Films which have Adsorbed Ethylene and Oxygen .....	59

CHAPTER 4 - SURFACE AREA DETERMINATIONS OF NICKEL FILMS WHICH HAVE ADSORBED MERCURY OR CAESIUM

PART 1 - NICKEL-MERCURY SURFACES

4.1.	Introduction .....	64
4.2.	Apparatus .....	65
4.3.	Experimental Procedure .....	65
4.4.	Direct Counting of Mercury Adsorbed by Film Surface ..	67
4.5.	Calculation of Amount of Mercury Adsorbed .....	68
4.6.	Counting of Radioactive Solutions .....	68
4.7.	Results and Discussion of Films which have Adsorbed Mercury .....	69
4.8.	Mercury Contamination as a Source of Error in Surface Area Determinations .....	71

PART 2 - NICKEL-CAESIUM SURFACES

4.9.	Introduction .....	72
4.10.	Experimental .....	73
4.11.	Experimental Procedure .....	74
4.12.	Results and Discussion of Caesium Adsorption Experiments .....	75

CHAPTER 5 - GAS ADSORPTION APPARATUS

5.1.	McLeod Gauges .....	81
5.2.	Construction of McLeod Gauges .....	85
5.3.	Gas Adsorption Apparatus .....	87
5.4.	Operation of Gas Adsorption Apparatus for Surface Area Determinations .....	88
5.5.	Chemisorption of Gases .....	89
5.6.	Protection of Catalyst Vessel from Mercury Vapour ....	90
5.7.	Storage of Gases .....	91
5.8.	The Purification of Hydrogen .....	94
5.9.	Preparation and Purification of Nitrous Oxide and Ethylene .....	95
5.10.	Preparation of Oxygen, Krypton, Xenon and Helium .....	96
5.11.	The Thermostat .....	96

CHAPTER 6 - PREPARATION OF NICKEL FILMS FOR ADSORPTION STUDIES

6.1.	Construction of Catalyst Vessel .....	98
6.2.	Treatment of Catalyst Vessel before Film Deposition ..	100
6.3.	Deposition of Nickel Films .....	102
6.4.	Estimation of Nickel .....	103

<u>APPENDIX A</u>	Derivation of the Expression used to Calculate the Volume of Krypton Adsorbed, and the Pressure at which this Adsorption Took Place .....	106
-------------------	---	-----

<u>APPENDIX B</u>	Calibration of McLeod Gauge .....	109
-------------------	-----------------------------------	-----

<u>APPENDIX C</u>	A Typical Surface Area Determination .....	110
-------------------	--	-----

<u>REFERENCES</u>	.....	115
-------------------	-------	-----

## SUMMARY

The adsorption isotherms of krypton on high vacuum evaporated nickel films and nickel films which have chemisorbed oxygen have been studied. The oxygenation of the clean nickel films was effected either by admitting pure oxygen to the surface directly or by allowing nitrous oxide to catalytically decompose on the surface. It has been shown that the decrease in the krypton monolayer value, which was calculated from the B.E.T. equation, was comparable for the chemisorption of oxygen by both methods of oxygenation, and that it cannot be satisfactorily explained by the mechanisms of thermal sintering, induced sintering, or pore blocking. It has been shown that the percentage decrease in the krypton monolayer value brought about by oxygen chemisorption was different from the percentage change in the xenon monolayer value, and it has been inferred that changes in the krypton monolayer value do not necessarily reflect a change in surface area. It has been suggested that this decrease in the krypton monolayer value might be explained by a surface dipole effect whereby the chemisorbed oxygen causes enhanced polarisation of the krypton atoms which would lead to increased lateral repulsion between the krypton atoms and hence to a decrease in the monolayer value.

The adsorption isotherms of chemisorbed layers of various types on nickel have been studied, viz. hydrogen, hydrogen and oxygen, ethylene, ethylene and oxygen, mercury, and caesium. These investigations revealed that the effect on the krypton monolayer value was independent of the direction of the induced dipole as would be expected if lateral repulsion were the cause of the  $V_m$  changes. Further it has been shown that when krypton is adsorbed on a surface which has chemisorbed two species one which has adsorbed positively and one which has adsorbed negatively, the polarising effect of these chemisorbed species tended to cancel, resulting in decreased lateral repulsion between the krypton atoms subsequently physically adsorbed.

The relationship between the coverage of a nickel surface with a chemisorbed species and the change in the krypton monolayer value has been studied using mercury and it has been shown that this relationship is linear until all available nickel sites are occupied.



## INTRODUCTION

For many years now it has been recognised that the phenomenon of heterogeneous catalysis arises from a surface process. The classical researches of Langmuir and Polanyi in 1916 and of Freundlich in 1923 established the connection between catalysis and adsorption, and the dependence of the rate of reaction on the extent of adsorption. The extent of the surface of the solid therefore influenced the rate at which the catalytic process occurred. Consequently catalysts were prepared in forms which would ensure a large surface area - either in a fine state of sub-division, or as highly porous particles.

Catalytic activity was later found to be dependent not only on the extent of the surface, but also, on the nature of the surface, that is on what have come to be known as geometric and electronic factors<sup>1</sup>. Surface area is therefore only one of the parameters which influence catalytic activity. In any fundamental investigation involving comparison of catalysts, it is

useful to have a measure of their surface areas, as this will facilitate, for example the distinction between promoters which affect the nature of the surface, and those which simply involve the maintenance of a large surface area.

The earliest attempts to measure surface area depended to a large extent on the irreversible chemisorption of such gases as hydrogen, carbon monoxide and oxygen. Benton<sup>2</sup> using carbon monoxide and hydrogen, and Emmett and Brunauer<sup>3,4</sup> using carbon monoxide showed that it was possible to obtain some measure of the surface area of various catalysts. Beeck<sup>5</sup> and co-workers and Rideal and Trapnell<sup>6</sup> tended to favour low temperature adsorption of carbon monoxide for measuring the surface area of thin metal films. This type of measurement differed from that of Emmett and Brunauer in that the low temperature adsorption of carbon monoxide was probably a mixture of both chemisorption and physical adsorption. A different method, not involving vacuum techniques, was suggested by de Boer and Dippel<sup>7,8</sup> who suggested measuring the surface area of certain materials, in particular calcium fluoride crystals, by the adsorption of water vapour.

Since these methods were dependent on chemisorption of gases, they were subject to uncertainty as to the extent and location of the adsorbed gas molecules. Thus the gas may not be chemisorbed on the entire surface but on only a portion of it, the so called active sites; or, on the other hand, in some cases it may have interacted with more than the outermost layer of atoms of the solid. In addition to this uncertainty, these methods suffered the disadvantage that the gases used to determine the surface area were irreversibly adsorbed, and in many cases poisoned the surface, so that comparative studies with other properties could not be made on the same catalyst specimen.

In many instances, particularly with industrial catalysts, this was not important. Indeed these methods were of advantage because they gave the sort of information which was more often wanted on industrial catalysts, because the number of chemisorption sites on a surface is more closely related to specific activity of a catalyst than is its surface area. On the other hand, in fundamental research where the surface areas of clean

catalysts, and those which had reacted, were desired, methods dependent on chemisorption techniques were unsatisfactory owing to the irreversible nature of the adsorption.

Since reversible adsorption was desirable, attention turned to the possibility of using low temperature physical adsorption measurement as a means of determining surface areas. Low temperature multi-layer physical adsorption of gases had the disadvantage that adsorption did not tend to a saturation value corresponding to a monolayer, so that it was impossible to determine directly what fraction of the total volume of gas adsorbed, was required to form a monolayer on the solid. Benton and White<sup>9</sup> while studying the low temperature adsorption of nitrogen by iron catalysts however observed a sharp break on the adsorption isotherm, which suggested to Emmett and Teller a possible method for measuring surface areas. They suggested that the sharp break in the adsorption isotherm might correspond to the completion of a first layer and the beginning of a second layer. If such a point could be found on an adsorption isotherm this

would then give a direct measure of the surface area, since the number of molecules adsorbed could be calculated from the volume required to form a monolayer, and it is only necessary to know the area of cross section of the adsorbing molecule to calculate the total area covered. This sharp break in the adsorption isotherm was called the point B, and the method developed by Brunauer, Emmett and Teller is known as the B.E.T. point B method. Even the B.E.T. point B method however, did not prove entirely satisfactory as a general method for measuring surface areas, since not all adsorption isotherms had a sharp break. For example the adsorption isotherm of n-butane on silica gel<sup>10</sup> is completely devoid of any point B, and in many other cases the method was rather uncertain owing to the difficulty of selecting the point B on the adsorption isotherm. To overcome this difficulty Brunauer, Emmett and Teller attempted to develop a quantitative theory of physical adsorption and this resulted in their theory of multi-layer adsorption and the B.E.T. equation<sup>11</sup>, which is essentially an extension to multilayer adsorption of Langmuir's theory of monomolecular adsorption. Using this equation, which is basically a mathematical method for determining the

point B, the volume of adsorbate required to form a monolayer can be calculated, even for those systems which do not have a sharp break on the adsorption isotherm. The B.E.T. plot has now become the standard method for measuring surface areas. Although the theoretical derivation of the equation has several shortcomings the greatest justification for the use of the method is that it gives reproducible results with different adsorbates.

Using this method to measure surface areas, several workers found that the chemisorption of certain gases by evaporated metal films caused a decrease in surface area. Klemperer and Stone<sup>12</sup> reported that chemisorption of oxygen by high vacuum evaporated nickel films caused a threefold decrease in surface area. A similar effect has been observed by Roberts<sup>13</sup> when oxygen was chemisorbed on evaporated iron films, a fivefold decrease in surface area resulting.

They explained this decrease in surface area by postulating that the heat evolved during chemisorption of the oxygen caused thermal sintering of the film. These

are not isolated instances, for example Bagg and Tompkins<sup>14</sup> reported that adsorption of carbon dioxide caused a decrease in the surface area of nickel films, and Tuzi OKamoto<sup>15</sup> reported a similar effect for oxygen on barium films. These workers also suggest that the decrease in surface area is caused by thermal sintering of the metal surface. Finally, Stone and Tiley<sup>16,17</sup> and Cannon<sup>18</sup> have all reported that chemisorption affects the surface area of a solid as measured by low temperature physical adsorption.

There seems to be considerable evidence that chemisorption of gases does in some way affect the surface area of a solid, but there is much doubt as to how the change arises. Most workers seem to tacitly agree that decreases in surface area are caused by sintering of the solid, due to the heat evolved during adsorption of the gases. There are several anomalies however, For example Roberts<sup>13</sup> reported that chemisorption of hydrogen by iron films caused an increase in surface area. Although the heat of adsorption and the coverage of hydrogen is less than that of oxygen some sintering should still occur, and therefore a decrease, small perhaps, should be observed, and certainly not an increase. Crawford Roberts and

Kemball<sup>19</sup> observed that the adsorption of ethylene, by nickel films caused a decrease in surface area comparable to that caused by the adsorption of oxygen, and yet the heat of adsorption and relative coverage of ethylene on nickel films is much less than that of oxygen. The same authors reported that hydrogenation of this adsorbed ethylene caused a similar decrease in surface area, although they calculated that the adsorption of ethylene would raise the temperature of the film by only 27°C, compared with 200°C in the case of the hydrogenation reaction. They suggest however that the heat of adsorption is more effective than the heat of hydrogenation for sintering, since none of the liberated heat will be transported away by the reactants. There is other evidence which suggests that the validity of this sintering hypothesis is questionable. For example it has been reported that chemisorption of oxygen by iron causes a five fold<sup>13</sup> decrease in surface area, whereas for nickel the decrease is threefold<sup>12</sup>, and yet at 25°C nickel sinters three times as fast as iron<sup>13,19</sup>.



Because of the failure of these attempts to explain many of the instances in which surface area changes, brought about by chemisorption, were observed, it was decided to design a series of experiments to try to decide whether the observed surface area decreases were genuine and caused by sintering, or possibly a steric effect, or whether they were apparent and caused by some other effects such as a surface dipole effect, or indeed by a flaw in the B.E.T. method itself.

## CHAPTER I

### Theoretical basis of the experimental method.

## INTRODUCTION

It is well known that in many cases when a

## CHAPTER I

### Theoretical basis of the experimental method.

## CHAPTER I

### Theoretical basis of the experimental method.

1.1

#### INTRODUCTION

It has been seen that in many cases when a gas was chemisorbed by a clean metal surface, a change in surface area resulted. In most instances this change was a decrease in surface area, which has been suggested by some workers to be caused by thermal sintering of the metal. It was decided to investigate more closely one of these systems, namely the nickel-oxygen system. This particular system was chosen for a closer investigation of the sintering hypothesis, as both the heat of chemisorption and coverage of oxygen on nickel are large. Since the rate at which oxygen is chemisorbed by a nickel surface is immeasurably fast a large rise in temperature of the nickel surface might be expected and consequently the conditions would be favourable for thermal sintering to occur.

Because the chemisorption of oxygen is instantaneous, the temperature rise of the nickel surface, and therefore the degree of sintering, will be controlled by the rate at which oxygen becomes available for chemisorption. If the nickel is oxygenated indirectly via nitrous oxide less sintering of the metal would be expected than if the nickel had been oxygenated by direct admission of oxygen, since the rate determining step in the chemisorption of the oxygen is the catalytic decomposition of the nitrous oxide.<sup>20</sup> In this case the heat would be liberated over a much longer period of time.

Accordingly experiments were designed to measure the surface area of clean nickel films, and nickel films which had oxygen chemisorbed on their surface. The chemisorption of oxygen was effected either by admitting oxygen directly to the surface, or by allowing nitrous oxide to catalytically decompose on the surface.

## 1.2 Measurement of Surface Areas.

Although Langmuir<sup>21</sup> in 1918 and later Baly<sup>22</sup> attempted to generalise the ideal localised monolayer treatment to include the formation of multi-molecular adsorbed films, it was not until 1938 that the mathematical difficulties were overcome and an equation of practical utility derived. The multi-molecular adsorption theory of Brunauer Emmett and Teller yields a useful two constant equation from which surface areas and approximate heats of adsorption can be calculated. Since it was proposed to use this technique to measure surface areas in this research, a discussion of the theoretical basis of this technique is therefore relevant.

In developing their theory of multilayer adsorption Brunauer Emmett and Teller<sup>11,23,24,25</sup> assumed that the surface was uniform, all sites having the same adsorption potential, and that the heat of adsorption of the second and higher layers was equal to the heat of liquefaction of the adsorbate gas. There is now much evidence to show that most surfaces are heterogeneous, and that the heat of adsorption only approaches the heat of liquefaction after at least three adsorbed layers have formed on the surface.

It was also assumed that the ratio of condensation coefficients in the first and higher layers was unity, whereas it has been calculated (Emmett<sup>26</sup>) that this ratio may differ from unity by a factor of 10 - 100.

These defects of the B.E.T. theory make it unlikely that the theoretical B.E.T. isotherm should ever correspond to an experimental isotherm. Nevertheless it is found that the B.E.T. equation is a good representation of a very large number of isotherms between the pressure range 0.05 - 0.35  $P_0$ , where  $P_0$  is the saturated vapour pressure of the adsorbate at the temperature of adsorption.

The most common adsorbates used in conjunction with the B.E.T. method to measure surface areas are nitrogen and krypton. Using liquid nitrogen as a coolant and gaseous nitrogen as the adsorbate several disadvantages are encountered. Firstly relatively high pressures of nitrogen, about 500 mm. of mercury, have to be used before a monolayer is formed. For small surface areas the amount of nitrogen physically adsorbed is therefore only a small fraction of that which remains in the gaseous state. The effect of this is to reduce the precision of the method, because the quantity being determined is obtained as a

difference between two relatively much larger experimentally measured quantities. Secondly Kokes and Emmett<sup>27</sup> have shown that nitrogen is "chemisorbed" by nickel to the extent of at least 28% of the total uptake of nitrogen. This "chemisorbed" nitrogen is only removed by prolonged pumping at room temperature (16 hours). This retention of nitrogen by thin films has also been observed by Beeck<sup>28</sup> and Trapnell<sup>29</sup>.

If krypton is used as the adsorbate, and liquid nitrogen as the coolant, the ratio of krypton in the gas phase to that on the surface is very much smaller, because lower pressures can be used owing to the smaller saturated vapour pressure of krypton at this temperature. The success of krypton can be judged from its wide application.<sup>30,31,32,33,34,35,36,37</sup>. Consequently in this research krypton was used in preference to nitrogen. A similar argument can be put forward, which leads to a stronger case, for the use of xenon. However as Anderson and Baker<sup>38</sup> pointed out prolonged pumping is required to remove the adsorbed xenon. Preliminary experiments showed that the B.E.T. plots obtained for  $P/P_0$  values of  $10^{-3}$  were linear. At values of  $P/P_0$  below  $5 \times 10^{-4}$  curvature of the B.E.T. plot was observed on several occasions. Heterogeneity seems a likely explanation of this phenomenon since Ehrlich and

Hudda<sup>39</sup> have shown that the inert gases, in particular xenon and krypton, are preferentially adsorbed round the 100 crystal face of tungsten. This phenomenon would be most noticeable at very low coverages.

Surface areas were not calculated from the uncertain direct readings of the point B method on the adsorption isotherms, but the volume  $V_m$  corresponding to unimolecular coverage was taken from the B.E.T. graph. The form of the B.E.T. equation used was:

$$\frac{P/P_o}{V(1-P/P_o)} = \frac{1}{V_m C} + \frac{(C-1)}{V_m C} P/P_o$$

where  $V$  is the volume adsorbed at pressure  $P$  mm.  $P_o$  is the saturated vapour pressure of krypton at the adsorption temperature. Experience showed that the constant  $C$  was about 1000 for clean films and about 400 for films which had oxygen chemisorbed on the surface, and since  $P \ll P_o$  in the range over which the measurements were made, the B.E.T. equation could be simplified to:

$$\frac{P/P_o}{V} = \frac{1}{V_m C} + \frac{P/P_o}{V_m}$$



Accordingly  $\frac{P}{P_0}$  was plotted against  $\frac{P}{P_0 V}$ , when a straight line of slope  $\frac{1}{V_m}$  was obtained.

It is obvious that, provided the pressure can be measured accurately, the lower the pressure range used the more sensitive is the surface area determination, since the ratio of the volume of krypton adsorbed to that in the gas phase increases with decreasing pressure.

It has normally been accepted that appreciable fractions of a monolayer are not formed by physical adsorption unless the value of  $P/P_0$  exceeds 0.01. Gains and Cannon<sup>40</sup> have however shown by calculation and experiment that with krypton as the adsorbate a monolayer is formed at much lower relative pressures. Roberts<sup>41,42</sup> has shown that krypton gives linear B.E.T. plots on evaporated iron films at  $P/P_0$  values as low as  $10^{-4}$ . In some cases certain adsorbents<sup>43</sup> will physically adsorb gases at  $P/P_0$  values as low as  $10^{-8}$ .

The value of  $P_0$ , the saturated vapour pressure of krypton, varies quite sharply with temperature. At  $-195^\circ\text{C}$  it is  $1.75 \text{ mm}^{44}$  whereas at  $-183^\circ\text{C}$  it is about  $10 \text{ mm}^{45}$ . It follows that for absolute surface area determinations

the temperature at which the adsorption takes place must be known accurately. However for relative surface areas the conditions are not so stringent, requiring only that the temperature should remain constant during any sets of measurements which were to be compared. This was accomplished by using the same sample of liquid nitrogen as the coolant, precautions being taken to prevent condensation of atmospheric oxygen into the sample, during the surface area determinations. It was calculated that the saturated vapour pressure of krypton, at the temperature at which the adsorption measurements were done  $81^{\circ}\text{K}$ , as measured with a butane thermometer, was 2.3 mm. As only relative values of film areas were required, and since there is some uncertainty as to the value of the cross-sectional area of the adsorbed krypton atom, areas were expressed in terms of the monolayer value  $V_M$  in  $\text{cm}^3$  mm. at  $300^{\circ}\text{K}$ .

To plot the B.E.T. graph it was necessary to know the volume adsorbed,  $V_e$ , for varying equilibrium pressures,  $P_e$ . The most usual method of determining these values is to allow several samples of krypton to condense on the surface and measure the equilibrium pressure after each

addition. This method would however involve a series of rather complicated gas pipettes which would increase the dead space as well as the manipulation. The method adopted was to admit krypton at the highest pressure it was desired to use, and to reduce the pressure stepwise by successive expansions into an evacuated standard volume. This gave a series of readings from which could be calculated the values necessary to draw the B.E.T. plot. An expression was developed to calculate the volume of krypton adsorbed,  $V_a$ , and the pressure,  $P_a$ , at which this adsorption took place. This expression and its derivation is shown in Appendix A.

### One Point Methods

The B.E.T. method of determining surface areas is very time consuming in that it is necessary to carry out a large number of adsorption measurements followed by a large number of calculations. It was therefore decided to examine some simplified methods of plotting the B.E.T. graph. Several simplified methods have been proposed by other workers.<sup>46,47,48,49</sup>

These so called "one point" methods all suffer the disadvantage that they tend to be inaccurate and although they may be of use in the fast determination of surface areas of industrial catalysts these methods

are not sufficiently accurate to measure the changes with which this work is concerned.

The method developed by Innes<sup>48</sup> depends on the equation:

$$V_m = 3.5 V_{0.2}$$

where  $V_m$  is the volume required to form a monolayer and  $V_{0.2}$  is the volume adsorbed at relative pressure of  $P/P_0 = 0.2$ . This relationship does not hold, even with reasonable accuracy, for high vacuum evaporated nickel films, since experiment has shown that the krypton monolayer is completed at relative pressure of  $P/P_0 \approx 1 \times 10^{-2}$ . If the above equation was used, in the estimation of the surface areas of evaporated nickel films, the areas obtained would differ from the  $V_m$  value from the B.E.T. graph slope by at least a factor of 3.

The method developed by Kell and co-workers depends on a simplification of a rearranged form of the B.E.T. equation:

$$\frac{1}{V(1 - \frac{P}{P_0})} = \frac{1}{V_m} + \frac{1}{V_m C} \left( \frac{1 - \frac{P}{P_0}}{\frac{P}{P_0}} \right)$$

according to the above author the last term in this equation becomes very small for values of C greater than 100, and therefore the equation becomes:

$$\frac{1}{V(1 - \frac{P}{P_0})} = \frac{1}{V_m}$$

This approximation only holds when the value of  $\frac{P}{P_0}$  approaches the maximum value permissible for B.E.T. measurements, that is 0.35. For very low values of  $\frac{P}{P_0}$ , that is about  $10^{-2}$ , a large error is incurred if the last term of the equation is neglected.

The most satisfactory one "point" method is that developed by Keil<sup>47</sup>

$$V = V_m \text{ when } \frac{P}{P_0} = \frac{1}{1 + \sqrt{C}}$$

this relationship follows from the B.E.T. equation.

The disadvantages with this method are essentially experimental. For a number of similar catalysts samples the value of C could be calculated for one sample using the B.E.T. equation, and the surface areas of the other

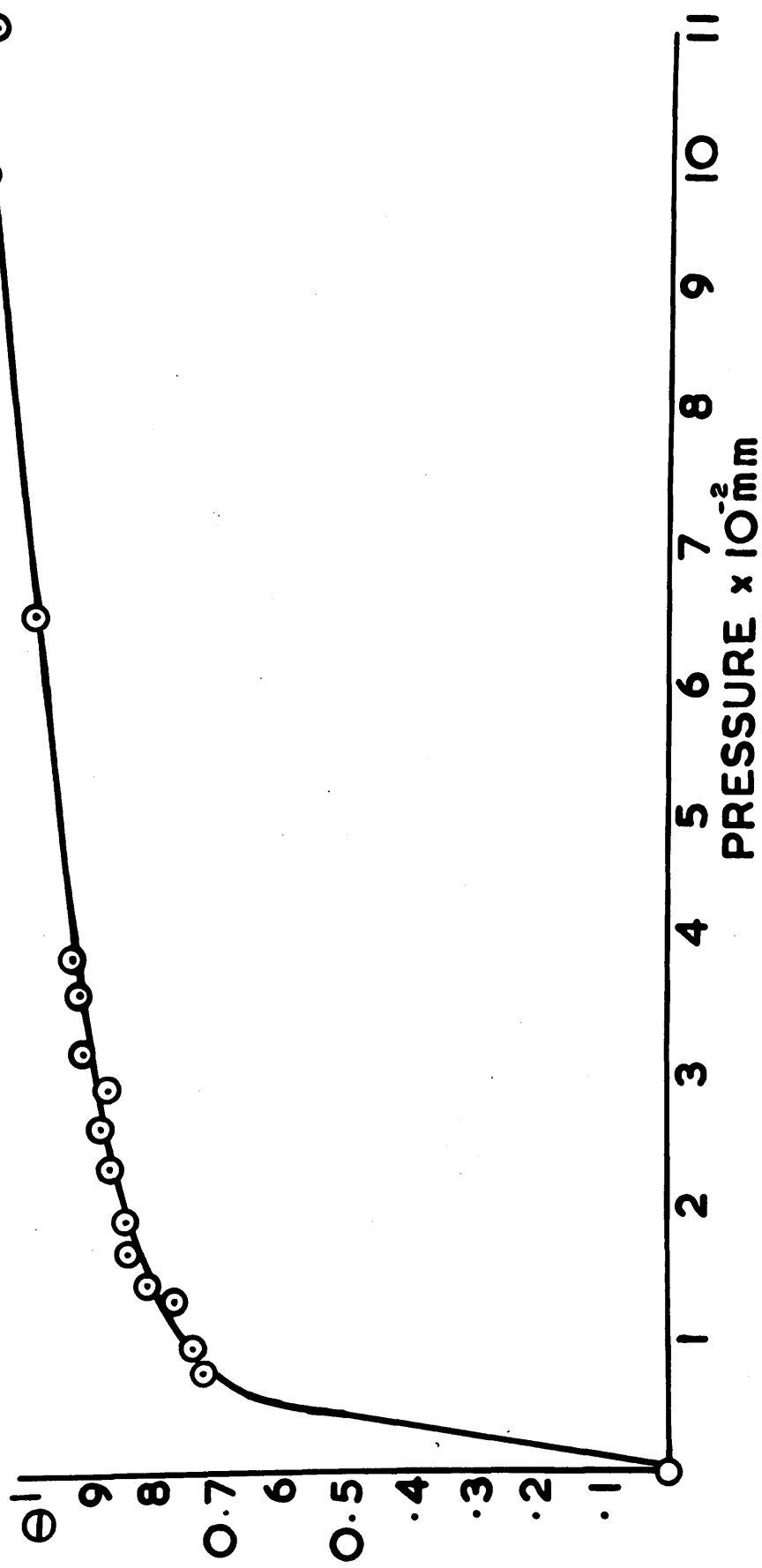
samples evaluated using the above equation. This involves measuring the volume of gas adsorbed at a predetermined pressure, which necessitates the use of a complicated gas pipette system, and this is undesirable from the point of view of dead space considerations, as has been mentioned previously.

#### 1.4 Independent "One Point" Method

As none of these "one point" methods was satisfactory, a method was developed which was independent of approximations of the B.E.T. method or empirical equations, but was based only on experimental evidence. The volume  $V_m$  necessary for the completion of a monolayer was calculated for a number of clean nickel films using the standard B.E.T. plot. The volume of gas adsorbed,  $V_a$ , at various pressures,  $P_a$ , was divided by  $V_m$  to give a series of values for surface coverage with respect to pressure, which gave a smooth curve as shown in fig.1. To calculate the surface area of any given film, a volume of gas was allowed to be adsorbed and the equilibrium pressure measured. From the graph the coverage at that pressure could be obtained and, knowing the volume adsorbed, the

Coverage of clean nickel film  
with krypton

FIG 1



volume required for complete coverage could be calculated. Table 1 compares the areas calculated by this method with those values calculated from the B.E.T. method, and shows that the accuracy is quite satisfactory.

TABLE 1

B.E.T.	ONE POINT	% diff.
82.0	86.0	4.9
73.0	77.0	6.1
65.0	66.5	2.3
65.2	65.2	0
65.0	66.2	1.6
112.0	108.0	3.5
77.0	75.7	1.5
71.0	67.5	4.3
72.8	71.8	1.4
76.4	77.0	0.8
75.0	75.0	0
61.65	62.6	1.6
45.0	44.1	2.0

The best accuracy reported for any of the other "one point" methods is 5%.



A similar graph of coverage plotted against pressure can be drawn for nickel surfaces covered with a chemisorbed gas. It was found however that for chemisorbed surfaces this "one point" method was not so accurate, and this led to the method being rejected for comparative measurements on clean and oxygen covered nickel films.

### 1.5 Thermal Transpiration

If at low pressures two parts of a system are at absolute temperatures  $T_1$  and  $T_2$  a pressure gradient is associated with the temperature gradient along the connecting tube. This effect is known as thermal transpiration or thermomolecular flow.

These conditions arose during the estimation of surface areas, since the catalyst vessel was at  $78^\circ\text{K}$  and the McLeod gauge was in a thermostat at  $300^\circ\text{K}$ . In addition, at the pressures of krypton used, the mean free path of the krypton atoms is of the same order as the diameter of the tubing which was in the temperature gradient. For accurate surface area determinations, correction must therefore be made for this effect.

Provided the bore of the tubing is very much smaller than the mean free path of the gas molecules Knudsen's<sup>50</sup> correction may be applied:

$$\frac{P_1}{P_2} = \sqrt{\frac{T_1}{T_2}}$$

Knudsen's relationship only holds good when  $\frac{d}{l} \ll 1$ , where  $d$  is the bore of the tubing and  $l$  is the mean free path of the molecules. Consequently application of this formulae to the pressures obtained in this research would result in a gross over correction.

The theoretical treatment of this effect when  $d \approx l$  is extremely difficult. The method of correction best suited to the conditions arising in this research is probably that of Porter<sup>51</sup>:

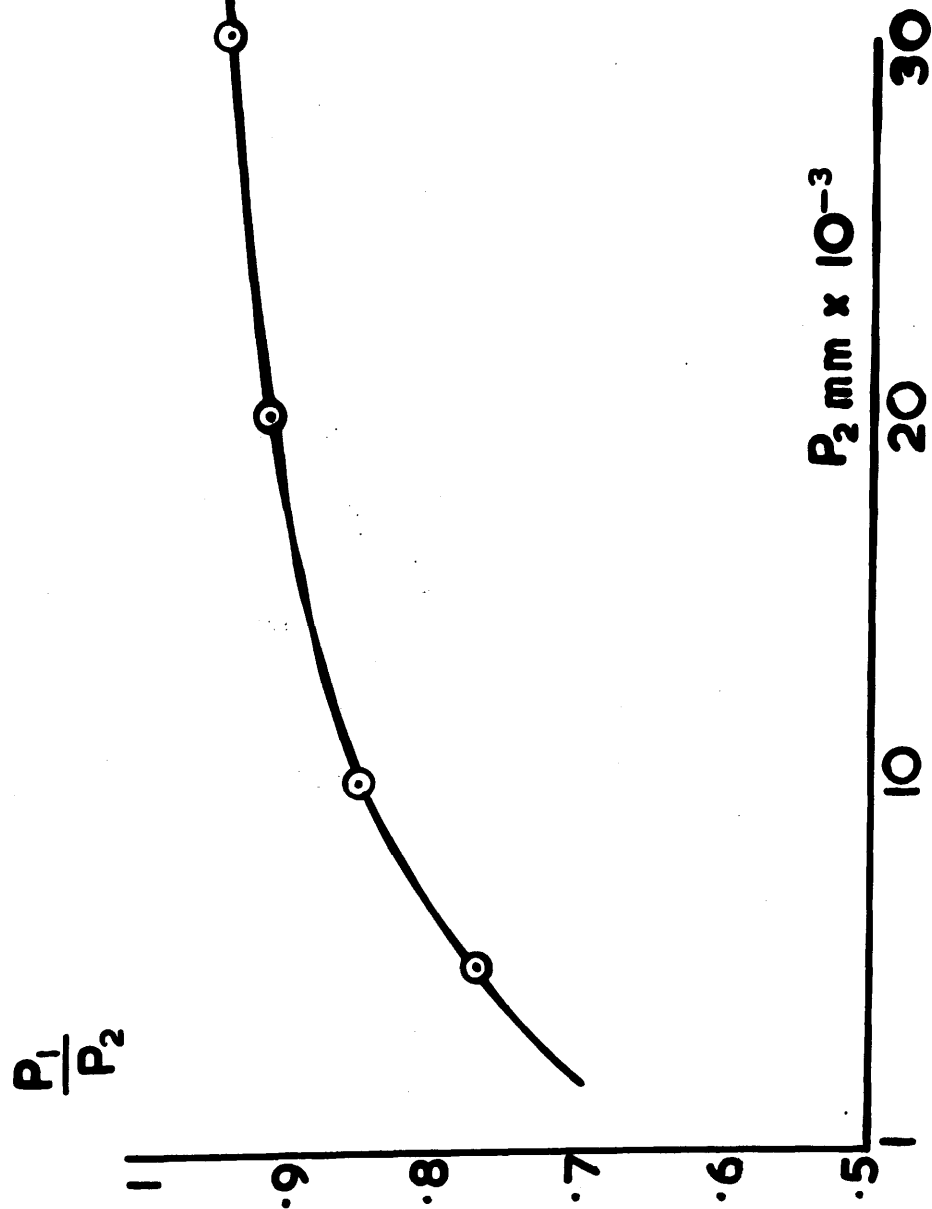
$$\frac{P_1}{P_2} = P_2 \left( \frac{C + (C^2 + 2CT_1/P_2 + T_1T_2/P_2^2)^{1/2}}{2CP_2 + T_2} \right)$$

where  $C = \frac{d \cdot 273}{10760}$

and  $l_0$  = mean free path of the gas molecule at N.T.P.

FIG. 2

Thermal transpiration corrections for krypton  
where  $\Delta T = 222^\circ\text{C}$ , and tube diameter = 1.3 cm.



Although application of this equation would also result in an over correction, it would give some idea of the magnitude of the effect. Accordingly this equation was used to calculate the ratio of  $\frac{P_1}{P_2}$  for varying pressures of krypton. These results are plotted in the form of a graph, fig. 2, and as can be seen the error at pressures above  $1 \times 10^{-2}$  mm, which was the lowest pressure normally used, is only 8%. It was decided to check this theoretical treatment experimentally. This was done by expanding varying amounts of krypton into a standard volume and measuring the resulting pressure. The effect of thermal transpiration was found to be very small in the pressure region in which the adsorption measurements were normally made. Experimental determinations of this effect have been made for krypton<sup>44,52,53,54</sup> and xenon.<sup>55</sup> Bennet and Tompkins<sup>56</sup> recommend the empirical method of correction of Liang.<sup>55,56,57,58</sup>

In view of the fact that both the theoretical and experimental determination showed that the effect of thermal transpiration was slight, and since only relative surface areas and not absolute areas were required, the method of correction adopted was that of cancellation of

errors, as used by Crawford Roberts and Kemball.<sup>19</sup>

This was accomplished by adjusting the initial amount of krypton admitted to the catalyst vessel so that the pressure range was the same for clean and chemisorbed films, consequently the correction for thermal transpiration would be the same in both cases, and could therefore be neglected.

## Surface Area Measurements on

## Oxygen and Nitrous Oxide Oxygenated Films

The apparatus was basically a high vacuum system which was constructed from wide-bore Pyrex tubing.

## CHAPTER II

### Surface Area Measurements on

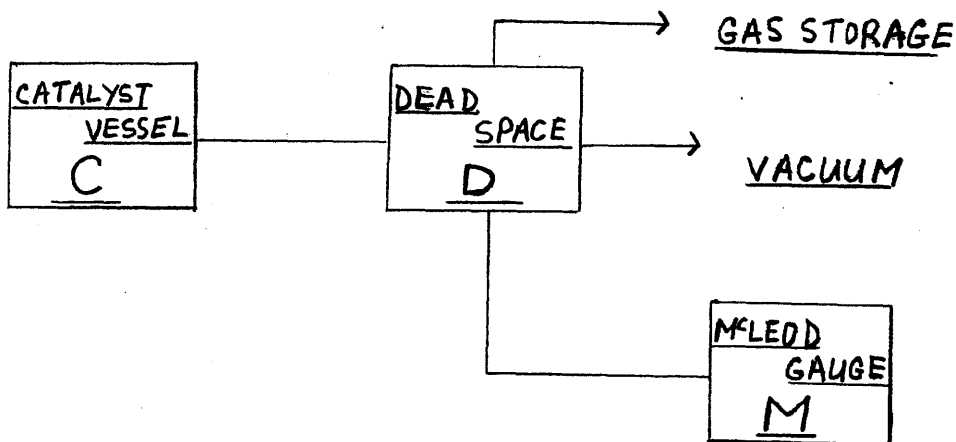
### Oxygen and Nitrous oxide Oxygenated Films

## CHAPTER II.

### Surface Area Measurements on Oxygen and Nitrous Oxide Oxygenated Films

#### 2.1 Apparatus

The apparatus was basically a high vacuum system and was constructed from wide-bore Pyrex tubing and wide-bore taps to ensure rapid evacuation. Vacuum was produced by using a two-stage mercury diffusion pump backed by an Edwards rotary pump. The gases to be used in the measurement were stored in two litre bulbs fitted with mercury cut-offs. These were used, rather than vacuum stopcocks, to enable gases to be stored for long periods without fear of contamination by air entering the apparatus owing to deterioration of the stopcock grease. All pressures were measured with McLeod gauges which were contained in a thermostat at 300°K. A detailed description of the construction and operation of the apparatus is given in Chapter V.



## 2.2 Results of Oxygen and Nitrous Oxide Oxygenated Films

Although film deposition and adsorption procedures were identical for all films, the reduction in  $V_m$ , brought by direct chemisorption of oxygen, varied considerably.

The values obtained for these films are shown in table 2, from which it may be seen that not only did the reduction in  $V_m$  vary from about 40% to 14%, but the amount of oxygen adsorbed per unit surface area, also varied. The values obtained for this quantity are however comparable with those of Klemperer and Stone<sup>59</sup> (1.70) and Brennan Hayward and Trapnell<sup>60</sup> (2.68). There does not seem to be any obvious relationship between this specific adsorption of oxygen and the



TABLE 2

Oxygen covered nickel films

FILM No.	FILM WEIGHT mg	Amount of oxygen chemisorbed	V <sub>m</sub> for clean film	V <sub>m</sub> after chemisorption	% Reduction in V <sub>m</sub> clean	Oxygen $\frac{V_m}{V_m \text{ clean}}$
26	19.94	199.9	71.5	39.6	44.2	2.80
17	35.22	130.0	72.6	54.0	25.6	1.79
32	26.85	189.2	75.0	55.4	26.1	2.52
34	17.07	164.0	61.7	50.0	19.0	2.66
35*	32.30	163.2	45.0	38.9	13.6	3.62
37	5.81	45.9	26.8	23.3	13.2	1.71
36	22.29	180.0	61.1	34.5	43.2	2.94
39	21.80	72.0	64.8	37.4	42.4	1.11

All quantities are in the unit  $\text{cm}^3 \text{ mm}$  at  $300^\circ \text{K}$

\*Film 35 pre-sintered at  $100^\circ \text{C}$  for one hour.

reduction in  $V_m$ .

The results for those films which were oxygenated indirectly, by allowing nitrous oxide to decompose on their surfaces, are shown in table 3. It was found that the activity of the films for decomposing nitrous oxide was lost after approximately half the amount of oxygen which would be expected to be taken up by direct oxygen chemisorption was adsorbed. The reduction in  $V_m$ , caused by this smaller amount of oxygen, was comparable with, indeed rather larger than, that in the direct oxygen adsorption.

In view of the considerable variation of  $V_m$  brought about by chemisorption of oxygen, it was decided to investigate the possibility of "ageing" effects, which might cause surface area changes of the film during the period in which it was being investigated. As the results in table 4 show the change in surface area caused by "ageing" was negligible over a period of six hours. It is to be emphasised that none of the adsorption measurements carried out on normal films was made until one hour had elapsed after film deposition, and similarly no adsorption measurements were made after seven hours had elapsed, so that any "ageing" which occurred would only have a small effect on the results.

TABLE 3

Nitrous oxide oxygenated films

FILM No.	FILM WEIGHT mg	Amount of N <sub>2</sub> O decomposed	Vm clean Film	Vm after chemisorption	% Reduction in Vm clean	Oxygen(O <sub>2</sub> ) Vm clean
20	47.80	362.4	125.0	68.2	45.5	1.45
31	30.76	212.0	76.4	58.0	24.2	1.39
9	10.40	-	57.1	33.8	40.9	-
10	17.20	-	67.2	37.6	44.0	-
12	22.70	108.2	62.8	26.0	58.6	0.86

All quantities are in the unit cm<sup>3</sup> mm. at 300°K.

TABLE 4

Time in hours	Vm
1	61.05
4	58.65
7	58.15

### 2.3 Discussion of results with oxygenated films

The outstanding feature of the results in tables 2 and 3 is the comparability of the decrease in  $V_m$  caused by the two methods of oxygenation. In the case of those films which were oxygenated by nitrous oxide, a smaller rise in temperature would be expected owing to the slower process of catalytic decomposition of the nitrous oxide, which would allow time for the efficient dissipation of the heat liberated by the subsequent chemisorption of oxygen. Because of this it is difficult to ascribe these changes in  $V_m$  to thermal sintering, where thermal sintering is understood to mean growth of elementary<sup>a</sup> crystallites due to an increase in temperature, caused by chemisorption.

Because of the variations in the values for the decrease in  $V_m$ , and for the amount of oxygen, relative to  $V_m$ , which was adsorbed, it was decided to construct graphs of krypton coverage vs. pressure, in the manner discussed in 1.4, for several of the films used. These graphs are shown in fig. 3 for the clean films and fig. 4 for the oxygen covered films. It can be seen that all the clean films are similar and consequently the variation in the decrease of  $V_m$  must result from the

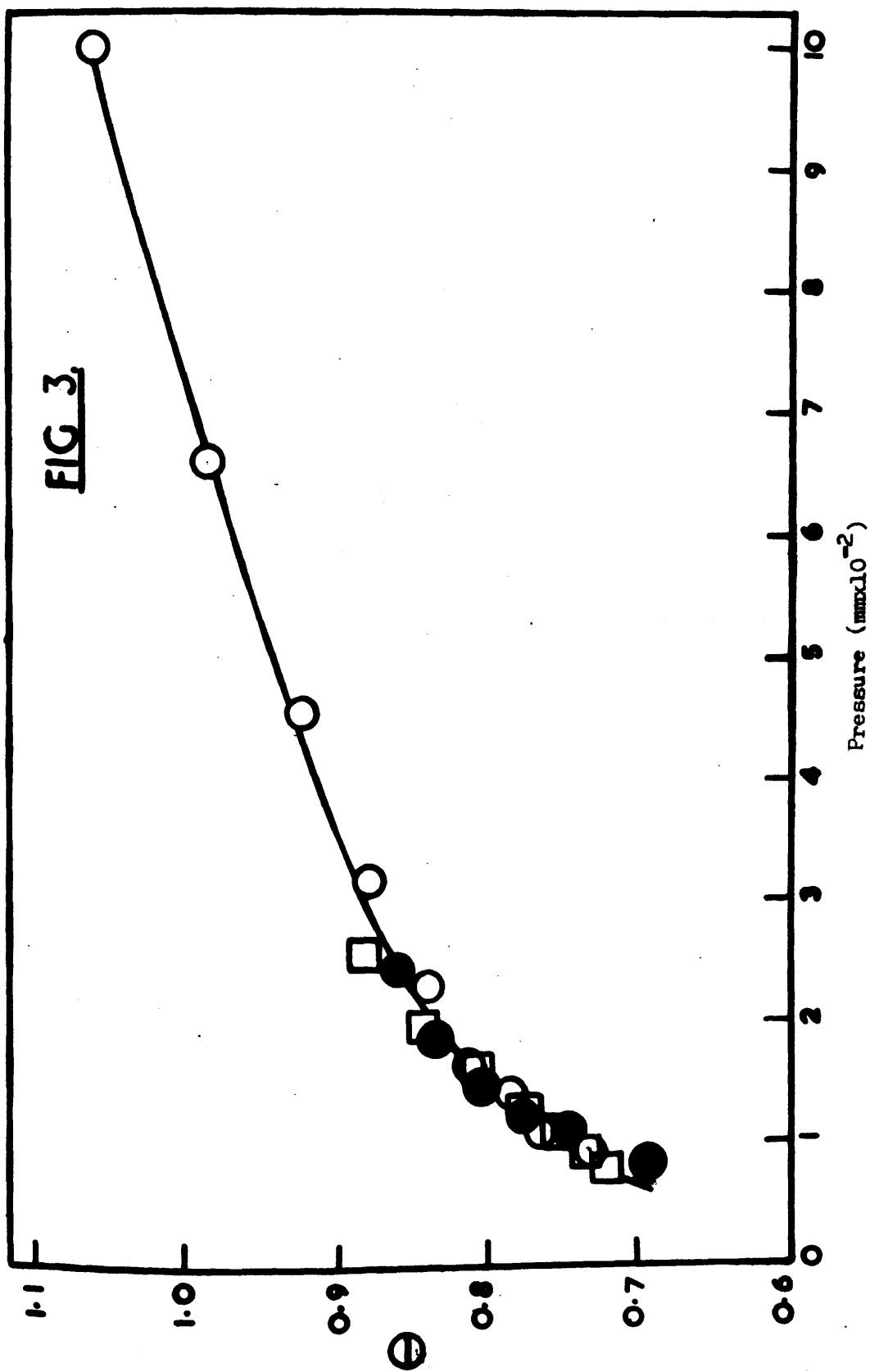


Fig. 3 - Krypton adsorption isotherms at  $78^{\circ}\text{K}$  on typical clean nickel films  
 Film 25,  $\circ$ ; Film 31,  $\bullet$ ; film 32,  $\square$ .

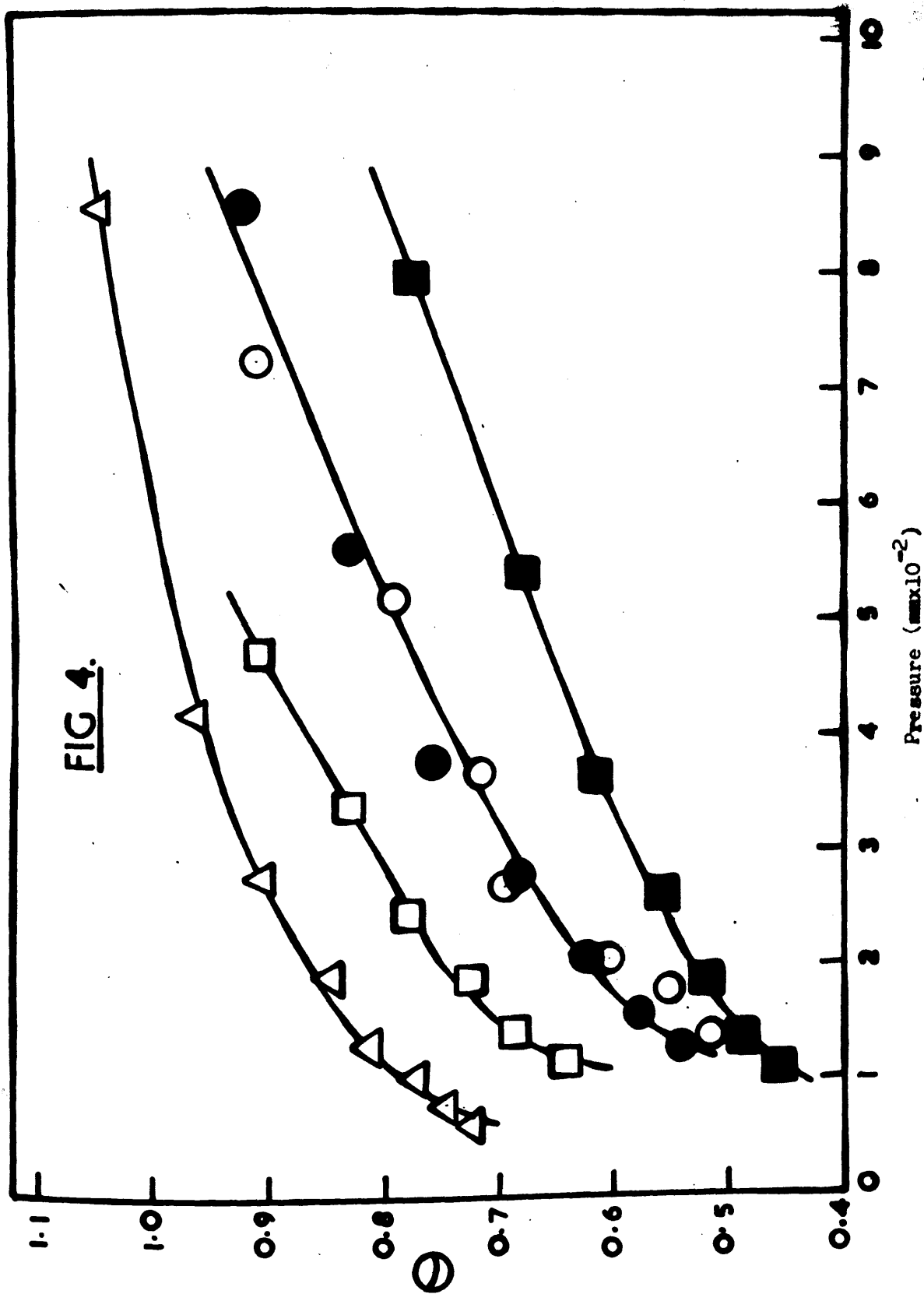


Fig. 4 - Krypton adsorption isotherms at 78°K for films upon which oxygen had been chemisorbed. Film 20, O<sub>2</sub>+N<sub>2</sub>O, ◻; film 26, O<sub>2</sub>, ○; film 31, N<sub>2</sub>O, ● and N<sub>2</sub>O + O<sub>2</sub>, ◻; film 32, O<sub>2</sub>, ◻.

chemisorption process, rather than differences which have resulted from variations in the method of preparation of the clean films.

The fact that the curves for clean and oxygen covered films are different suggests that the decrease in surface area is apparent rather than genuine. In general it is seen that for a given pressure of krypton, the coverage of a chemisorbed film is less than that for a clean film.

It was decided to look at the kinetics of the thermal sintering process to determine if the large decrease in surface area observed was even theoretically possible.

The nickel films used in this investigation adsorbed on average  $1.95 \times 10^{17}$  atoms of oxygen per mg of nickel. Since the heat capacity of nickel is about 0.1 cal/gm., and since the heat of chemisorption of oxygen on nickel is about 140 K cal/mole, chemisorption of oxygen would cause a rise in temperature of about 225°C. if none of the heat was lost from the film.



$1.95 \times 10^{17}$  atoms of oxygen adsorbed per mg. of nickel

$\therefore \frac{1.95 \times 10^{17}}{2 \times 6.03 \times 10^{23}}$  moles of oxygen per mg. of nickel

$$\begin{aligned} \therefore \text{Heat liberated} &= \frac{1.95 \times 10^{17}}{6.03 \times 10^{23}} \times 140 \times 10^3 \text{ cal.} \\ &= 2.265 \times 10^{-2} \text{ cal.} \end{aligned}$$

$$M.S.\Delta T = 2.265 \times 10^{-2}$$

M = Mass of nickel = 1 mg.

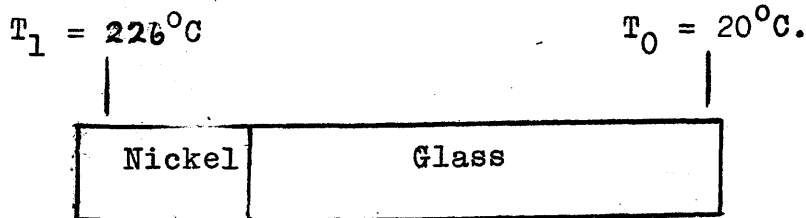
$$\begin{aligned} \Delta T &= \frac{2.265 \times 10^{-2}}{1 \times 10^{-3} \times 0.1} \\ &= 226^\circ\text{C.} \end{aligned}$$

S = Specific heat of  
nickel = 0.1 cal/gm.

$\Delta T$  = Temperature rise.

If this temperature was maintained for some time extensive sintering would occur.

In order to obtain some idea of the rate at which the nickel film cools, the following simple model was considered.



Let  $T$  = temperature after  $t$  secs.

Total heat given out by nickel between zero time and time

$$t = MS (T_1 - T)$$

Total heat given out by nickel at time  $(t + dt) = MS(T_1 - T - dT)$

∴ Heat lost in time interval  $dt = MSdT$

∴ Rate of loss of heat at time  $t = \frac{MSdT}{dt}$

$$\therefore \frac{MSdT}{dt} = \frac{-KA(T - T_0)}{D}$$

$K$  = coefficient of conductivity  
of glass.

$$\text{ie } \frac{dT}{dt} = \frac{-KA}{MSD} (T - T_0)$$

$A$  = area of contact of glass

$$\int_{T_1}^T \frac{dT}{T - T_0} = \frac{-KA}{MSD} \int_0^t dt$$

and nickel

$D$  = thickness of glass

$M$  = mass of nickel

$S$  = specific heat of nickel

$$\text{Then } \left[ \log_e (T - T_0) \right]_{T_1}^T = \frac{-KA}{MSD} t$$

$$\therefore \log \frac{T - T_0}{T_1 - T_0} = \frac{-KA}{MSD} t$$

$$\therefore t = \frac{-MSD}{KA} \log_e \frac{T - T_0}{T_1 - T_0}$$

This is an exponential function and therefore  
the half time for the rate of cooking can be calculated

$$\begin{aligned} \therefore \frac{t_1}{2} &= \frac{-MSD}{KA} \log_e \frac{1}{2} & M &= 1 \times 10^{-3} \text{ gm} \\ & & S &= 1 \times 10^{-1} \\ \therefore \frac{t_1}{2} &= -8 \times 10^{-4} \frac{\log \frac{0.5}{10}}{0.4343} & D &= 1 \times 10^{-1} \text{ cm} \\ & & K &= 2.5 \times 10^{-3} \\ &= 5.55 \times 10^{-4} \text{ secs.} & A &= 5 \text{ cm}^2 \end{aligned}$$

In this calculation it has been assumed that equilibrium between the glass and nickel has been reached. That is to say, a temperature gradient across the glass has been established. If allowance was made for the amount of heat required to establish this temperature gradient, the half time, for the rate of cooling of the nickel, would be even shorter.

In practise the oxygen was admitted to the nickel surface in three samples and not as one large amount. This would of course cause less sintering than if the oxygen had been admitted in one large sample.

From the result of previous calculation, a cooling curve for nickel deposited on glass has been constructed. This is shown in fig. 5, and it can be seen that the film would have cooled to  $10^\circ\text{C}$  above ambient in  $2.6 \times 10^{-3}$  secs. Comparing this time with the figure of  $1.7\% \text{ min.}^{-1}$  obtained by Crawford Roberts and Kemball<sup>19</sup>,

**FIG 5**

**Cooling curve for nickel deposited on glass**

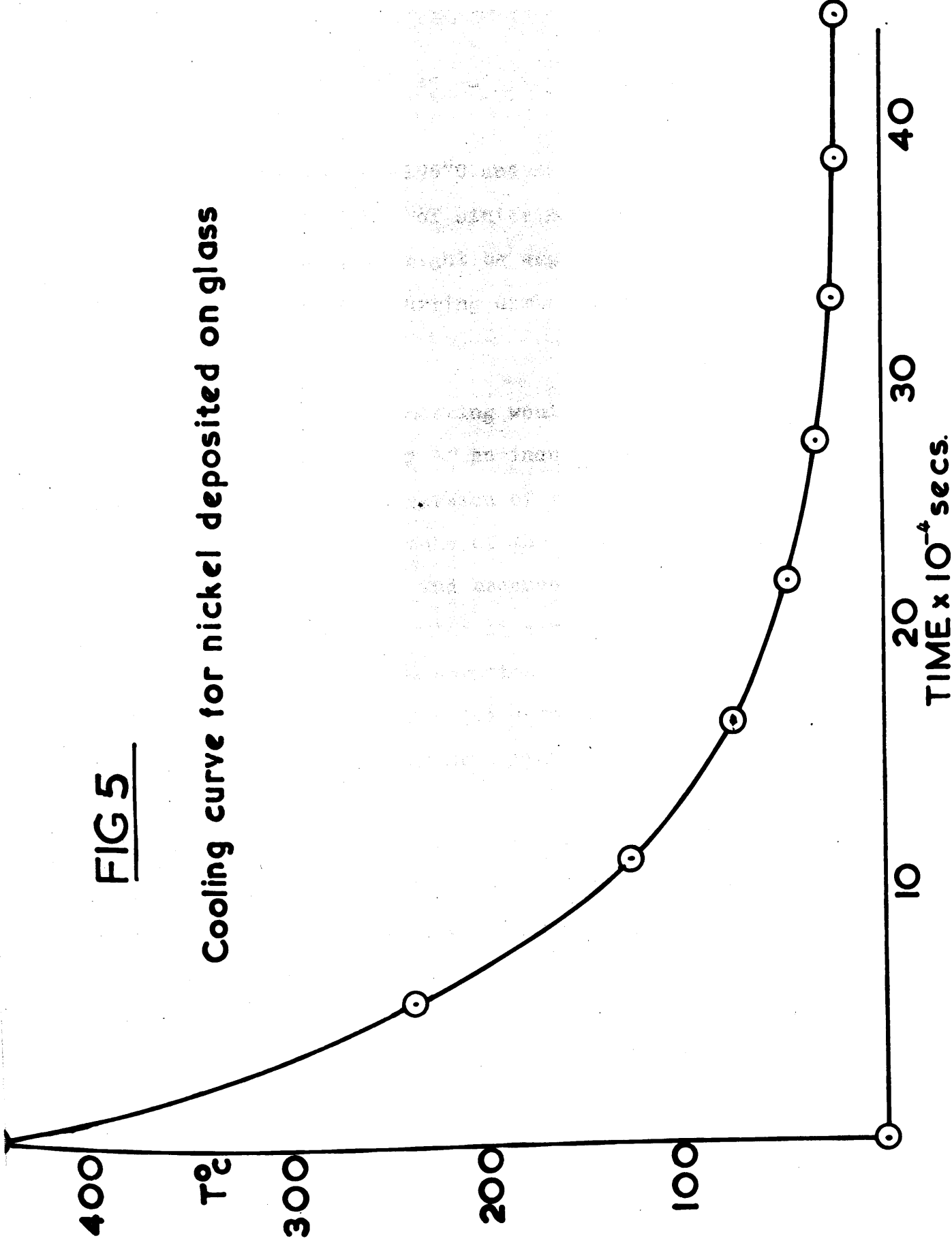
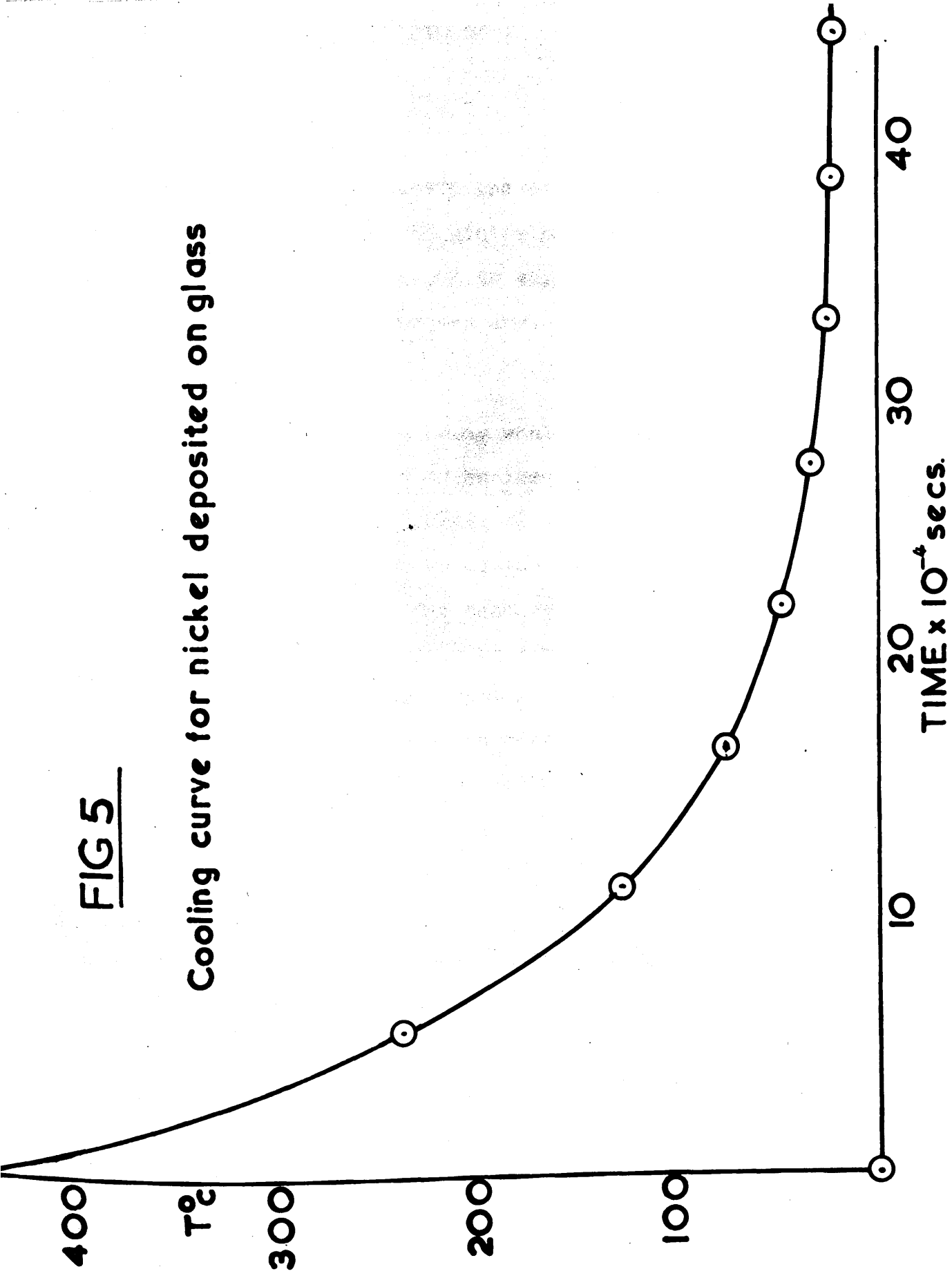


**FIG 5**

**Cooling curve for nickel deposited on glass**



for films deposited at  $-195^{\circ}\text{C}$  and sintered at  $25^{\circ}\text{C}$ , and noting that the rate of sintering for films at  $100^{\circ}\text{C}$  is not much greater, it might be expected that the amount of thermal sintering occurring during chemisorption would be negligible.

Although thermal sintering would appear to be unlikely, the possibility of an induced form of sintering, caused by the direct conversion of the energy of adsorption, must be considered. Because of the unusual features of the structure of metals, and because of what is sometimes referred to as free valencies at a metal surface, it is possible that the chemisorption process might involve a transition state in which the adsorbed molecule is associated with more than one surface atom. If such a transition state occurs during chemisorption it is possible that the surface atoms might undergo rearrangement. Supporting evidence for this possibility comes from the work of Jech<sup>61</sup> who noted that a platinum surface labelled by ion-bombardment with radon or radioactive xenon, released activity when certain gases were allowed to be chemisorbed on its surface. Anderson<sup>62</sup> has also suggested that the energy liberated during adsorption might assist the migration of surface atoms.

It might be the case that the results for the nickel films oxygenated via nitrous oxide, which gave reductions in  $V_m$  larger than those in the case of oxygen, are in support of this mechanism of induced sintering, for although the heat of adsorption is liberated more slowly, giving rise to a smaller temperature increase, the total energy output is greater by 36 Kcal/mole of oxygen adsorbed, the heat of dissociation of nitrous oxide. However because of the variation of both the nitrous oxide and oxygen results it is doubtful whether such significance can be claimed for them.

#### 2.4 Results and discussion of films which have been oxygenated by both oxygen and nitrous oxide.

The results for these films are shown in table 5. It was found that a film which had decomposed nitrous oxide would adsorb a further amount of oxygen. This additional amount of oxygen was equal to about half of that already present on the film. It was found however that nitrous oxide would not decompose on a film which had previously been saturated with oxygen. The oxygen adsorbed by the nitrous oxide films was

TABLE 5

Nitrous oxide decomposition followed by oxygen adsorption on same nickel film.

FILM No.	FILM WEIGHT mg.	Amount of Nitrous oxide decomposed	Amount of oxygen chemisorbed	Vm of clean film	Vm after N <sub>2</sub> O	Vm after N <sub>2</sub> O + O <sub>2</sub>	% change in Vm	Oxygen(O <sub>2</sub> ) Vm. clean	Ratio O from N <sub>2</sub> O: O from O <sub>2</sub>
20	47.8	362.4		125.0	68.2		45.5	1.45	2.21
			81.9	125.0		50.0	60.0	2.10	
		212.0		76.4	58.0		24.2	1.39	
31	30.76		52.7	76.4		50.6	33.8	2.08	2.02

All quantities are in the unit cm<sup>3</sup> mm at 300°K.



associated with a further decrease in surface area. This decrease was however not directly proportional to the additional amount of oxygen adsorbed, but was rather less.

Zettlemoyer<sup>63</sup> and co-workers have suggested that when oxygen is chemisorbed by a nickel film, a layer of nickel oxide results on top of which is a half layer of negatively charged oxygen ions. It might well be then, that this additional amount of oxygen adsorbed by the nitrous oxide film is being used to build up this second layer of oxide, and therefore <sup>does</sup> not cause such a marked decrease in  $V_m$ .

## 2.5 General Discussion

It has been shown that there is considerable doubt as to whether thermal sintering or an "induced" form of sintering could cause the surface area decreases observed. The smaller than average decrease in surface area, table 2, observed for film 35, which was sintered at 100°C for 30 mins. might be considered to be evidence in favour of an induced form of sintering, since the pre-sintering of the film would have smoothed

out the nickel surface, and therefore subsequent migration of the surface atoms caused by the heat of adsorption, would not have such a marked effect. Although the decrease in  $V_m$  was smaller than the average, it was still within the limits of those values for the other films and therefore it is doubtful if this significance can be attached to the result.

It is of interest to note the results obtained by Brennan, Hayward and Trapnell<sup>60</sup> on manganese films. These films were found to adsorb oxygen, and this uptake of oxygen was accompanied by a decrease in the surface area of the film. On being allowed to stand these films were found to be able to adsorb a further quantity of oxygen, and it was found that their surface area had increased above the value it had reached during the initial oxygen adsorption. Since the effect of sintering could only be to cause a decrease in surface area, these observations show that in this case at least there are other factors of greater magnitude determining the surface area change.

It is possible that the results of Brennan, Hayward and Trapnell could be interpreted by a steric or pore blocking effect. If in a metal film there were pores or fissures so narrow that the entry of krypton atoms was just marginally possible, it is likely that oxygen chemisorbed on these sites would deny entry to krypton atoms in a subsequent surface area determination. After standing for some time it was possible that some of the chemisorbed oxygen diffused into the bulk metal and therefore some of these fine pores would once more be accessible to krypton atoms, which would result in an increase in surface area.

A similar argument could be put forward for the result of film 35. The pre-sintering of this film would tend to smooth out the smaller pores in preference to the larger pores, so that the surface presented to the chemisorbed oxygen would be essentially made up of large pores with intervening stretches of "smooth surface", and therefore oxygen chemisorption would not be so likely to cause pore blocking. It is worth noting that although film 35 adsorbed about the same quantity of oxygen as

other films of comparable weight, a much higher pressure of oxygen was required before the surface became saturated. This equilibrium pressure for the sintered film was  $1.2 \times 10^{-2}$  mm. whereas for non sintered films it was about  $1.9 \times 10^{-4}$  mm.

If a nickel surface was made up of fine pores so narrow, that the entry of krypton atoms was just permissible, it is probable that if oxygen <sup>were</sup> chemisorbed on these sites it would prevent entry of krypton atoms in a subsequent surface area determination. It was proposed to test this idea by doing B.E.T. determinations of the clean and oxygen covered surface, using krypton and xenon in turn.

As the results in table 6 show, the change in surface is different depending on which of the gases is used in the surface area determinations. Assuming values of  $19.0 \text{ \AA}^2$  and  $24.0 \text{ \AA}^2$  <sup>64</sup> for the areas of cross section of krypton and xenon, absolute values for the surface area can be calculated from the measured monolayer values. As can be seen from table 6, these figures are in good agreement, which indicates that there is no

TABLE 6

Adsorbate	Clean Film		Oxygen chemisorbed film	
	V <sub>m</sub>	Area cm <sup>2</sup>	V <sub>m</sub>	% Reduction
Kr	72.6	4427	54.0	25.6
Xe	57.2	4395	51.0	10.8

All quantities are in the unit cm<sup>3</sup> mm. at 300°K.

part of the clean surface available to krypton which is not accessible to xenon. This suggests that the pore structure of the film is such that chemisorption of oxygen by this surface would not cause steric interference in subsequent physical adsorption.

The surface area decrease caused by chemisorption of oxygen if genuine, whatever the reason, would be expected to be the same whether estimated using krypton or xenon. As is shown by table 6 this is not so. It is therefore tentatively suggested that these changes in surface area caused by chemisorption of oxygen are apparent rather than genuine.

### CHAPTER III

The adsorption of krypton by nickel films  
on which hydrogen and oxygen has been  
chemisorbed, and on which ethylene and  
oxygen has been chemisorbed.

### CHAPTER III

The adsorption of krypton by nickel films on which hydrogen and oxygen has been chemisorbed, and on nickel films on which ethylene and oxygen has been chemisorbed.

#### 3.1 Introduction

It was evident from the experiments discussed in Chapter II that the mechanisms of thermal and induced sintering and the blocking of fine pores did not explain satisfactorily the observed decrease in  $V_m$  when oxygen was allowed to be chemisorbed by an evaporated nickel film. Consequently alternative explanations must be considered.

From the experiments in which both krypton and xenon were used as adsorbates it was tentatively concluded that the surface area decrease was apparent rather than genuine. It is therefore proposed to assume that the decrease in surface area is apparent and then to consider possible explanations for the observed decrease in  $V_m$ . At the same time the previously discussed mechanisms of thermal and induced sintering, and pore blocking will be borne in mind while this problem is being investigated.



It has been shown in Chapter I that the B.E.T. plots for both clean, and chemisorbed surfaces were linear in the pre-monolayer region. Roberts<sup>13</sup> also observed this linearity in the pre-monolayer region for both clean and chemisorbed iron films. It has been assumed by some workers<sup>13</sup>, that because the B.E.T. plots for clean and chemisorbed surfaces were both linear, the B.E.T. method could be used to compare their surface areas. Mignolet<sup>65</sup>, Pritchard<sup>76</sup> and Tompkins<sup>66</sup> have all shown that the presence of a chemisorbed layer affects the adsorption of the inert gases. The chemisorbed species seemed to affect the induced dipole on the inert gas atom, hence the phenomenon was most noticeable with xenon which is relatively easily polarised. It can be seen then, that a chemisorbed layer, apart from the more obvious effects it might have on the adsorption of krypton atoms, such as a simple steric effect or pore blocking, it also affects the nature of the adsorption of the krypton atoms in a more subtle fashion. It was thought that these less obvious changes in the mode of adsorption of the krypton might explain the decrease in  $V_m$  caused by the chemisorption of oxygen by nickel films.

### 3.2 The Surface Dipole Mechanism.

When physical adsorption of krypton takes place at a nickel surface, the forces involved in bonding the first layer of krypton to the surface are of two types:

- (a) van der Waals forces
- (b) electrostatic forces.

The van der Waals forces are the forces which cause multilayer adsorption. The electrostatic forces, which arise from polarisation of the adsorbate induced by the electrical double layer present at the nickel surface, are only of importance in the first layer of adsorbed krypton, the effect being very small in the second layer and almost negligible in the third layer.

From surface potential measurements<sup>66</sup> it is known that when oxygen is adsorbed by nickel it accepts an electron and becomes negatively charged. Effectively this means that the nickel surface is now obscured by a localised negatively charged oxygen array. Subsequently adsorbed krypton atoms will come in contact with this negatively charged surface which will polarise the krypton atoms to a greater extent than the clean surface.

Because of this enhanced polarisation of the krypton atoms, and because all the krypton atoms are polarised in the same direction, there will be an increase in lateral repulsion between the krypton atoms. This means that the krypton atoms will not approach each other as closely on a nickel-oxygen surface as they do on a clean nickel surface. In other words the area occupied by a krypton atom on a nickel-oxygen surface is greater than that on a clean nickel surface. This results in a  $V_m$  value for krypton on a nickel-oxygen surface which is less than that on a clean nickel surface.

If the chemisorbed oxygen causes increased polarisation of the krypton atoms, this should be seen as an increase in the heat of adsorption of krypton, since the electrostatic contribution to the binding forces will now be greater. The theory is therefore supported by the work of Ponc and Knor<sup>67</sup> who found that the heat of adsorption of krypton on nickel was increased by the presence of chemisorbed oxygen.

It was found however in this research that the value of  $C$  in the B.E.T. equation decreased when oxygen

was chemisorbed by a nickel film. The value of  $C$  is given by the expression

$$C = \frac{a_1 b_2}{a_2 b_1} \exp (E_1 - E_L)/RT$$

where  $E_1$  = Heat of adsorption in first layer

$E_L$  = Heat of adsorption in higher layers,

taken to be equal to the latent heat of evaporation.

The observed decrease in the value of  $C$  would therefore seem to imply that the heat of adsorption of krypton in the first layer had decreased. In calculating heats of adsorption from the B.E.T. equation, the assumption is made that the pre-exponential factor is equal to unity, and is independent of the heat of adsorption. The statistical derivation 68, 69 of the B.E.T. equation yields

$$C = j_s/j_L \exp (E_1 - E_L)/KT$$

where  $j_s$  and  $j_L$  are the partition functions for all internal degrees of freedom for a molecule in the first adsorbed layer and in the liquid state respectively,

and  $\epsilon_1$  and  $\epsilon_L$  are the potential energies of a molecule in the first layer and liquid respectively.

From this it appears that

$$\frac{a_1 b_2}{a_2 b_1} = \frac{j_s}{j_L}$$

Although the number of degrees of freedom in the first layer and higher layers is the same, the partition functions will differ. If it is assumed that  $j_L$  is constant, an increase in the heat of adsorption of krypton will cause a decrease in the values of  $\frac{j_s}{j_L}$  which may more than compensate for the increase in the exponential factor.

However, Hill<sup>70</sup> has noted that  $\epsilon_L$  is not synonymous with the latent heat of evaporation,  $L$ , of a liquid, and has defined a factor  $R$  by

$$C = R \exp \left[ (\epsilon_1 - L)/KT \right]$$

$R$  and  $a_1 b_2 / a_2 b_1$  are not identical. In the use of the B.E.T. equation to derive heats of adsorption it is thus strictly  $R$ , and not  $a_1 b_2 / a_2 b_1$  which is being set equal to unity.

From theoretical treatments Cassie<sup>68</sup> has calculated that R should have a value of  $\frac{1}{50}$  or less, whereas Hill<sup>70</sup> has calculated that R should have a value from 5 - 10. From experimental evidence the values obtained for R varied over several orders of magnitude. Kemball and Schreiner<sup>71</sup> have shown that R may in fact vary from  $2 \times 10^{-6}$  for toluene on mercury<sup>72</sup>, to 11 for xenon on mercury.<sup>73,74</sup> Finally the discrepancies between the B.E.T. heats of adsorption and the experimental values noted by Gregg and Jacobs<sup>75</sup> could only be accounted for by assuming that R varies in an unpredictable manner. It can be seen then that the assumption that R is unity is unreasonable, and that there is every possibility that the pre-exponential term R is the determining factor in the calculation of c values from the B.E.T. equation, so that an observed decrease in the value of C does not necessarily imply that the heat of adsorption has decreased.

It has been postulated that chemisorbed oxygen causes increased polarisation of the krypton atom. It is therefore relevant to discuss the surface potential

change which occurs when inert gases<sup>are</sup> adsorbed by clean and chemisorbed surfaces, since this is a measure of the change in the electrostatic field present at the surface, which in turn is related to the dipole moment of the adsorbed atom. It has been observed that physical adsorption of xenon results in a surface potential change of +0.85V on clean nickel<sup>65</sup> and +0.514V on copper<sup>76</sup>. This change in surface potential has been explained by no-bond<sup>77</sup> transference of electrons to the metal surface, or by the polarisation<sup>65</sup> of the xenon atom. Pritchard<sup>76</sup> has shown that the surface potential change when xenon is adsorbed on copper is +0.514V, whereas on copper which has chemisorbed oxygen the surface potential change is only +0.25V. At first sight it might be concluded from this observation that the xenon was not so strongly polarised as on the clean film. On closer examination however, it is apparent that any polarisation of the adsorbed xenon or krypton is likely to involve electron interactions between the inert gas and the oxygen layer, rather than between the inert gas and the metal. Any change in electrostatic potential brought about by the adsorption of the inert gas will not be completely passed on to the nickel, but will be retained

to a large extent by the oxygen array. Since the change in surface potential is a measure of the change in the electrostatic potential between a point outside the surface and a point in the bulk nickel, it does not follow that increased polarisation of krypton or xenon on a nickel-oxygen surface should be accompanied by an increase in the surface potential change.

In calculating the areas of xenon and krypton atoms, by comparison with nitrogen by adsorption experiments on the same surface, it has been found that, if the area of the nitrogen molecule is assumed to remain constant, that different areas have to be assumed for the krypton and xenon. These areas varied with the different adsorbents used. For krypton<sup>80,81,82,83,84,85</sup> the areas varied from 19.0 Å to 22.6 Å and for xenon<sup>86</sup> they varied from 18.2 Å to 27.3 Å. It is to be noted that not only is the variation in area large, but that the areas, which have to be assumed, are greater than those determined from liquid or solid density.<sup>80</sup> It was thought that this might be evidence in favour of the surface dipole mechanism.



### 3.3 Electron transfer mechanism

An alternative view of the positive surface potential observed when xenon is adsorbed by nickel, is that an electron is partially transferred from the xenon to the nickel. Consider now a nickel surface covered with chemisorbed oxygen. It might be argued that the electron transfer from the xenon to the chemisorbed surface would be more complete than on the clean surface, owing to the large electron affinity of the oxygen. This would mean that the net charge on the xenon atoms would be greater on the nickel-oxygen surface than on the clean surface, which would result in a greater repulsion between the xenon atoms, and this would result in a decrease in  $V_m$ .

It was to obtain more information about these mechanisms, and to confirm the conclusions which have been drawn concerning thermal sintering, induced sintering, and pore blocking, that the following experiments were designed. These experiments were in two series. The first of these consisted of measurements of the surface area of clean nickel films, films which had hydrogen chemisorbed on their surfaces,

and films which had hydrogen and oxygen chemisorbed on their surfaces. The second series was similar in every respect except that ethylene was used in place of hydrogen.

### 3.4 Results and discussion of hydrogen adsorption experiments.

As can be seen from table 7, chemisorption of hydrogen did not cause a decrease in the value of  $V_m$ . In the case of film 22, chemisorption of hydrogen caused an increase in  $V_m$  of 23.9%. Crawford Roberts and Kemball<sup>19</sup> have noted that chemisorbed hydrogen did not alter the value of  $V_m$  for a nickel surface. On the other hand Roberts<sup>13</sup> observed that, with iron films, chemisorbed hydrogen caused an increase in the volume of krypton adsorbed. This increase, which was of the order of 20%, decreased as higher pressures of krypton were used.

The results in table 7 can not be explained by thermal sintering, induced sintering, or pore blocking, since the effect of these could only be to cause a decrease in  $V_m$ , so that whether or not these mechanisms are important, there are certainly other factors of greater magnitude determining the change in  $V_m$ .

TABLE 7

Hydrogen Covered Surface

Film No.	Film Weight mg.	VM clean surface	Amount of hydrogen adsorbed	VM of hydrogen surface	%Change in VM
22	30.59	87.3	67.8	108.2	+23.9
23	31.05	65.0	64.1	65.0	0

All quantities are in the unit  $\text{cm}^3\text{mm}$  measured at  $300^\circ\text{K}$

To explain his results on iron films Roberts<sup>13</sup> postulated that the presence of chemisorbed hydrogen caused an increase in the heat of adsorption of krypton. He suggested that this increased heat of adsorption explained the increased adsorption of krypton in the pre-monolayer region. If this increase in the heat of adsorption of krypton was due to increased polarisation of the krypton there would only be enhanced adsorption of krypton at low coverages. At higher coverages, adsorption of krypton would be depressed owing to the increased repulsion between the similarly polarised krypton atoms. Consequently, it might be expected that, except at low coverages, an increase in the heat of adsorption would suppress the adsorption of krypton, whereas Roberts<sup>13</sup> found that adsorption of krypton was enhanced until a monolayer of krypton was completed.

As was explained in 1.2, because of the large value of  $C$  in the B.E.T. equation, the slope of the B.E.T. plot, from which  $V_m$  was calculated, was independent of the heat of adsorption, so that an

increase in the heat of adsorption of krypton would not result in an increase in the value of  $V_m$ , but at low coverages would simply increase the amount adsorbed at a given pressure.

It was therefore thought that a surface dipole mechanism similar to that proposed in 3.2 for oxygen adsorption might explain this increase in  $V_m$ . Owing to the small size of the hydrogen atom, which accepts an electron from the nickel, it can fit in between the surface nickel atoms. This means that the "free" surface electrons are now localised on the surface, and not above the surface as in the clean nickel film. The result of this would be the attenuation of the electrical double layer usually present at a metal surface. When krypton atoms come in contact with this surface, the electrostatic field strength of which has been diminished, the polarisation of the adsorbed krypton will be decreased. Consequently there will be less lateral repulsion between krypton atoms on a nickel-hydrogen surface than on a clean nickel surface, so that the area occupied by each krypton atom will have decreased, necessitating an increase in the value of  $V_m$  to cover the same area.

Whereas it has been postulated that the change in surface potential caused by the adsorption of xenon on an oxygen covered metal was not a direct measure of the dipole moment of the xenon, this postulate will not hold for a nickel-hydrogen surface. Unlike an oxygen covered surface, the adsorbed xenon will be virtually on the metal surface since the small hydrogen atom will have little steric effect. This then means that the surface potential change observed when xenon is adsorbed by a hydrogen covered metal should be a measure of the dipole of the xenon, or alternatively the quantity of charge transferred from the xenon.

Pritchard<sup>76</sup> has measured the surface potential change when xenon is adsorbed by gold and copper films. For clean gold and copper the surface potentials were +0.500V and +0.580V respectively, and for hydrogen covered surfaces they were +0.495V and +0.565V. These figures would seem to indicate that the xenon was not so strongly polarised on the hydrogen covered surface. It is inferred that the same would be true for a nickel-hydrogen surface.

### 3.5 Results and discussion of hydrogen and oxygen covered films

As can be seen from tables 8 and 9, chemisorption of oxygen on films which had already chemisorbed hydrogen caused a decrease in the value of  $V_m$ . This decrease taken as a percentage of the nickel-hydrogen surface is comparable with the decrease in  $V_m$  caused by the chemisorption of oxygen on a clean nickel film. This suggests that neither thermal nor an induced form of sintering is the cause of this decrease, since it is generally accepted<sup>13</sup> that chemisorbed hydrogen stabilises a metal surface to subsequent rearrangement of the metal surface atoms. Consequently a hydrogen covered surface should sinter less readily than a clean surface. As can be seen from table 10, the presence of presorbed hydrogen does not seem to affect the amount of oxygen which adsorbed, as this is comparable with the values for clean nickel films, table 2, Chapter II.

A nickel surface which has adsorbed hydrogen and then oxygen has probably the same geometry as a nickel surface which has adsorbed oxygen alone.

TABLE 8

Hydrogen and Oxygen Covered Films

Film No.	VM clean	Amount of hydrogen adsorbed	VM of hydrogen surface	Amount of Oxygen adsorbed	VM of hydrogen and oxygen surface.
22	87.3	67.8	108.2	253.7	71.2
23	65.0	64.1	65.0	162.0	45.1

All quantities are in the unit  $\text{cm}^3$  mm measured at  $300^\circ\text{K}$



TABLE 9

Hydrogen and Oxygen Covered Films

Film No.	% change in VM clean caused by adsorption		% change in VM of hydrogen surface caused by oxygen adsorption
	H <sub>2</sub>	O <sub>2</sub>	
22	+23.9	-18.45	-34.2
23	0	-30.80	-30.8

All quantities are in the unit cm<sup>3</sup> mm measured at 300°K

TABLE 10

<u>Hydrogen and Oxygen Covered Films</u>					
Film No.	VM clean	$\frac{\text{Amount of H}_2}{\text{VM clean}}$	$\frac{\text{Amount of O}_2}{\text{VM clean}}$	VM hydrogen surface	$\frac{\text{Amount O}_2}{\text{VM hydrogen surface}}$
22	87.3	0.78	2.90	108.2	2.42
23	65.0	0.98	2.49	65.0	2.49

Whereas before adsorption of oxygen the krypton atoms were adsorbed on a nickel surface, after oxygen adsorption the krypton atoms would be in contact with a localised negatively charged oxygen array. As explained in 3.2, this would lead to enhanced polarisation of the krypton atoms and increased lateral repulsion, and would result in a decrease in the value of  $V_m$ . It would seem that as far as krypton adsorption is concerned, there is no difference between an oxygen covered nickel surface, and one covered with both hydrogen and oxygen, owing to the similar distribution of charge on these surfaces, and possibly also the the special positions occupied by the adsorbed hydrogen.

### 3.6 Results and discussion of films which have adsorbed ethylene

The results in table 11, which are in good agreement with those of Crawford, Roberts and Kemball<sup>19</sup>, show that adsorption of ethylene caused a decrease in the value of  $V_m$ , the volume of krypton required to form a monolayer. This decrease in  $V_m$  was comparable to that caused by chemisorption of oxygen, even although both the heat of adsorption and the amount of ethylene

TABLE IIEthylene Covered Films

Film No.	Film weight mg.	VM for clean surface	Amount of ethylene adsorbed	VM for ethylene surface	Change in VM as a % of clean surface	Amount of $C_2H_4$ VM (clean)
24	37.78	112.60	-	66.20	-41.2%	-
25	29.42	77.0	40.98	38.70	-49.7%	0.53
27	40.44	114.20	45.00	72.80	-34.5%	0.40
28	22.26	72.80	39.60	50.50	-31.4%	0.54

All quantities are in the unit  $cm^3$  mm measured at  $300^\circ K$

adsorbed was less, which is further evidence against an explanation in terms of sintering, either thermal or induced.

Infra-red studies of films of adsorbed ethylene on nickel have shown that there is some uncertainty with regard to the mode of adsorption and the coverage of the surface. It is reasonably clear however that the adsorption in some way involves the double bond of the ethylene. Surface potential<sup>65</sup> measurements indicate that negative charge is transferred from the ethylene molecule to the nickel surface. After adsorption of ethylene a nickel surface has therefore a localised layer of positively charged "ethylene molecules". This positively charged layer of adsorbed ethylene, owing to the large size of the ethylene molecule, projects above the nickel surface, and is therefore unlike the adsorbed hydrogen which was incorporated in the surface. It is conceivable that this positively charged ethylene array will polarise subsequently adsorbed krypton atoms to a greater extent than a clean nickel film. Consequently there will be increased lateral repulsion between the krypton atoms which as has been shown already (3.2) will cause a decrease in

the value of  $V_m$ . The direction of the dipole on the krypton induced by contact with ethylene will of course be opposite to that induced by oxygen, this however is immaterial, since similarly aligned dipoles will always repel each other.

### 3.7 Results and discussion of krypton adsorption measurements on films which have adsorbed both ethylene and oxygen.

From table 12 it can be seen that associated with the adsorption of oxygen by films which had presorbed ethylene there was, in all but one case, an increase in the krypton  $V_m$  above the corresponding value for the nickel ethylene surface. In contrast with the case of oxygen on a hydrogen covered surface, presorbed ethylene suppressed the subsequent adsorption of oxygen.

The results in table 12 indicate that the final value of  $V_m$  for the surface depends both on the amount of ethylene and on the amount of oxygen adsorbed. More correctly, it seems that the final  $V_m$  value depends on the ratio of oxygen to ethylene present on the surface. Initially it seems that adsorption of oxygen causes an increase in the value of  $V_m$ , but as increasing amounts of the oxygen are added this increase in  $V_m$  becomes

TABLE 12

Ethylene and Oxygen Covered Films

Film No.	Film weight mg.	VM clean surface	Amount of ethylene adsorbed	VM ethylene adsorbed	Amount of Oxygen adsorbed	VM ethylene oxygen surface	Change in surface area		Amount $O_2$ VM (clean)	Amount $O_2$ Amount $C_2H_4$
							% clean surface	% ethylene surface		
25	29.44	77.0	41.0	38.7	129.8	47	-39	+21.5	1.69	3.17
27	40.44	114.2	45.0	72.8	204	54	-52.6	-25.8	1.79	4.54
28 <sup>a</sup>	22.26	72.8	39.6	50.5	73.2	58.6	-19	+16	1.02*	1.83
28 <sup>b</sup>	22.26	72.8	39.6	50.5	131.4	52.7	-27.7	+ 4.35	1.8	3.3

All quantities are in the unit  $cm^3$  mm measured at  $300^\circ K$

\*Not saturated with oxygen

smaller and eventually changes to a decrease. This is especially noticeable with film 28 where the first amount of oxygen adsorbed caused an increase in  $V_m$  of 16%, whereas adsorption of a further quantity of oxygen caused this increase to fall to 4%. It is inconceivable that any form of sintering, whether thermal or induced, could bring about an increase in the value of  $V_m$ . It is likewise, unlikely that pore blocking could cause such an increase.

When oxygen<sup>65,78,79</sup> is adsorbed by a nickel surface it becomes negatively charged whereas under the same circumstances ethylene becomes positively charged<sup>65</sup>. When oxygen is adsorbed by a nickel surface which has already adsorbed ethylene, it is reasonable to suppose that space will be available for the oxygen to be adsorbed in between the ethylene molecules, because the size of these ethylene molecules is such that adsorption cannot occur on adjacent pairs of nickel sites<sup>87</sup>. When are krypton atoms adsorbed by this composite surface of positively charged ethylene and negatively oxygen, it will be polarised with the positive end of the dipole pointing away from the surface if it is held above an ethylene molecule, while it will be polarised in the



opposite sense if it is in contact with an adsorbed oxygen atom. The situation now arises whereby there are two types of adsorbed krypton atoms, polarised in opposite directions to one another. This would of course lead to an attraction between some of the adsorbed krypton atoms, which would in turn lead to a reduction in the average area of surface occupied by each krypton atom. The result of this would be an increase in the value of  $V_m$ . It will be apparent that the magnitude of this increase in  $V_m$  will depend on the relative amounts of ethylene and oxygen on the surface. As the amount of oxygen on the surface increases, more of the adsorbed krypton will be polarised in the same direction and so what was originally predominantly an attractive force between oppositely polarised krypton atoms will become a repulsive force as the surface population of similarly polarised krypton atoms increases, and so the value of  $V_m$  would start to decrease again. Since the quantity of oxygen adsorbed is more than twice the quantity of ethylene adsorbed it is reasonable that the  $V_m$  value for a nickel surface saturated with ethylene and oxygen could be less than that for an ethylene covered surface.

In other words, on a surface which has been saturated with both oxygen and ethylene it is possible that the kryptons atoms would be more strongly polarised than they were on the ethylene surface, and consequently there would be a greater repulsion between them, which would result in an even greater decrease in  $V_m$ .

Alternatively, instead of considering the krypton atoms as being polarised by two different electrostatic fields due to the ethylene and oxygen the combined field might be considered. As oxygen is adsorbed the magnitude of the positive field, due to the presorbed ethylene, decreases until zero field is reached. After this point further adsorption of oxygen causes the sign of the field to change and the field strength once more increases.

Both of these models lead to the conclusion that adsorption of oxygen on a nickel-ethylene surface should initially cause an increase in the value of  $V_m$ , and that this should be followed by a decrease in the value of  $V_m$ . This is in perfect agreement with the observed results given in table 12.

**FIG 6**

1 - CLEAN FILM  
 2 - ETHYLENE FILM  
 3 - ETHYLENE-OXYGEN FILM

**FILM 25**

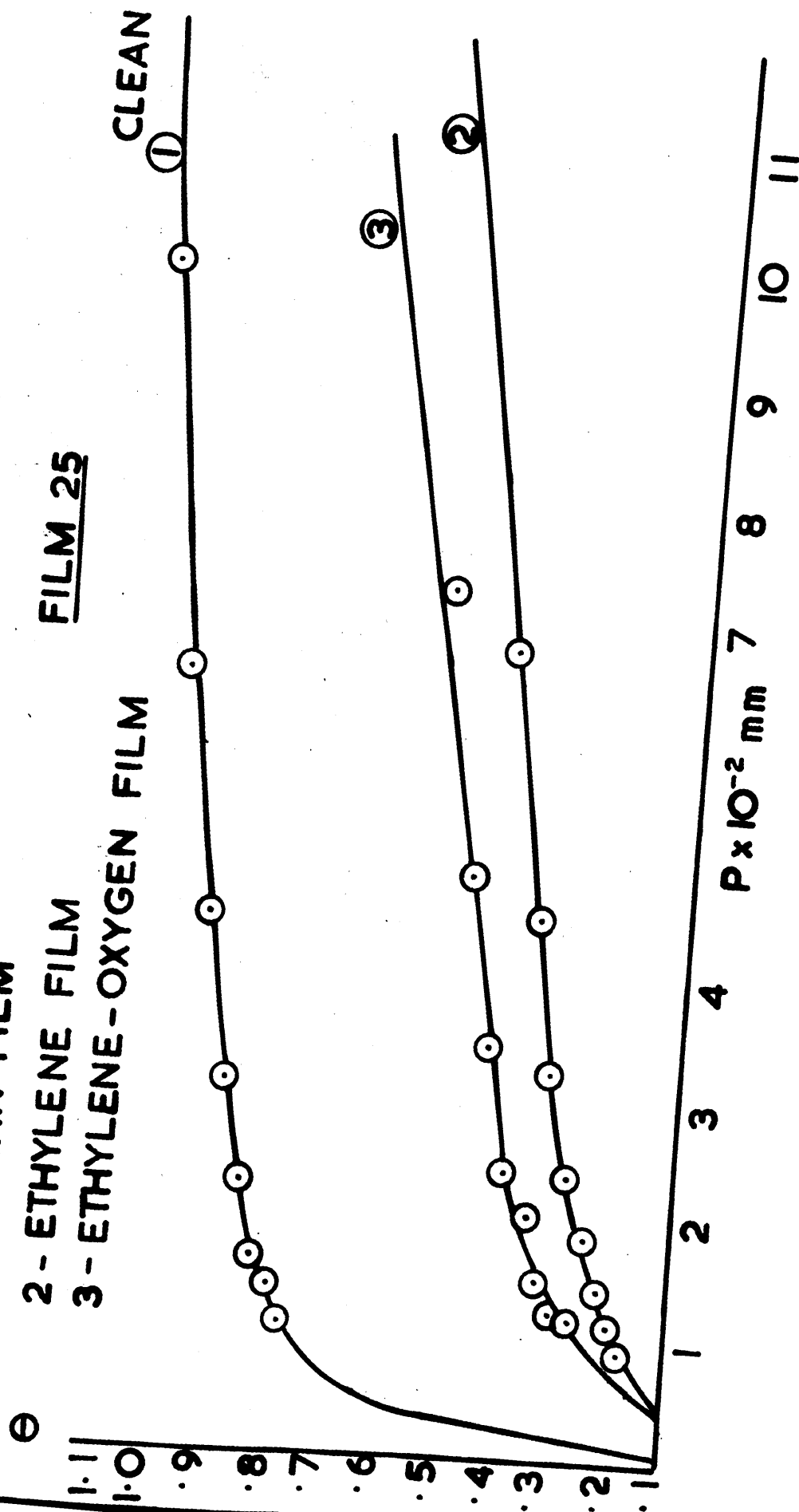


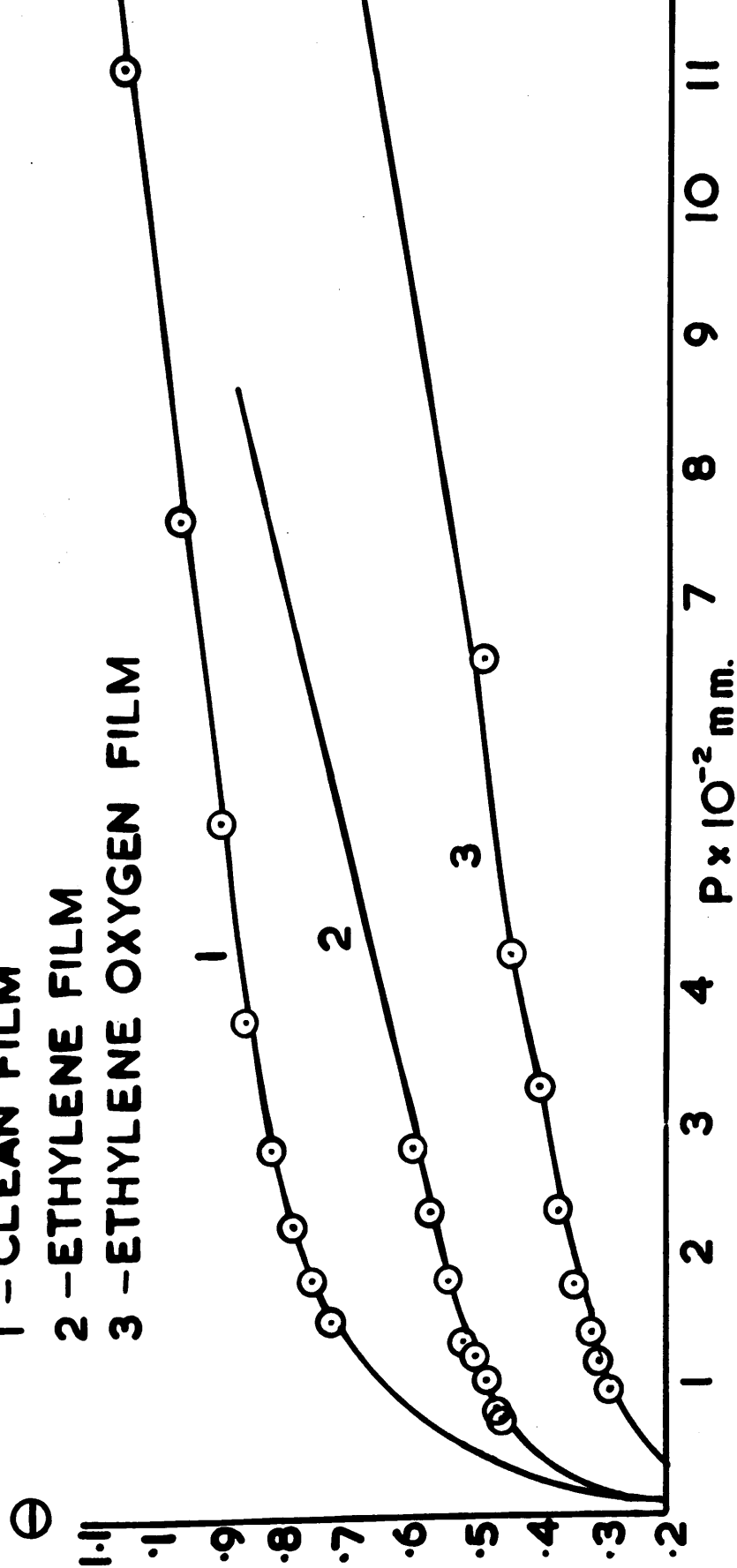
FIG. 7

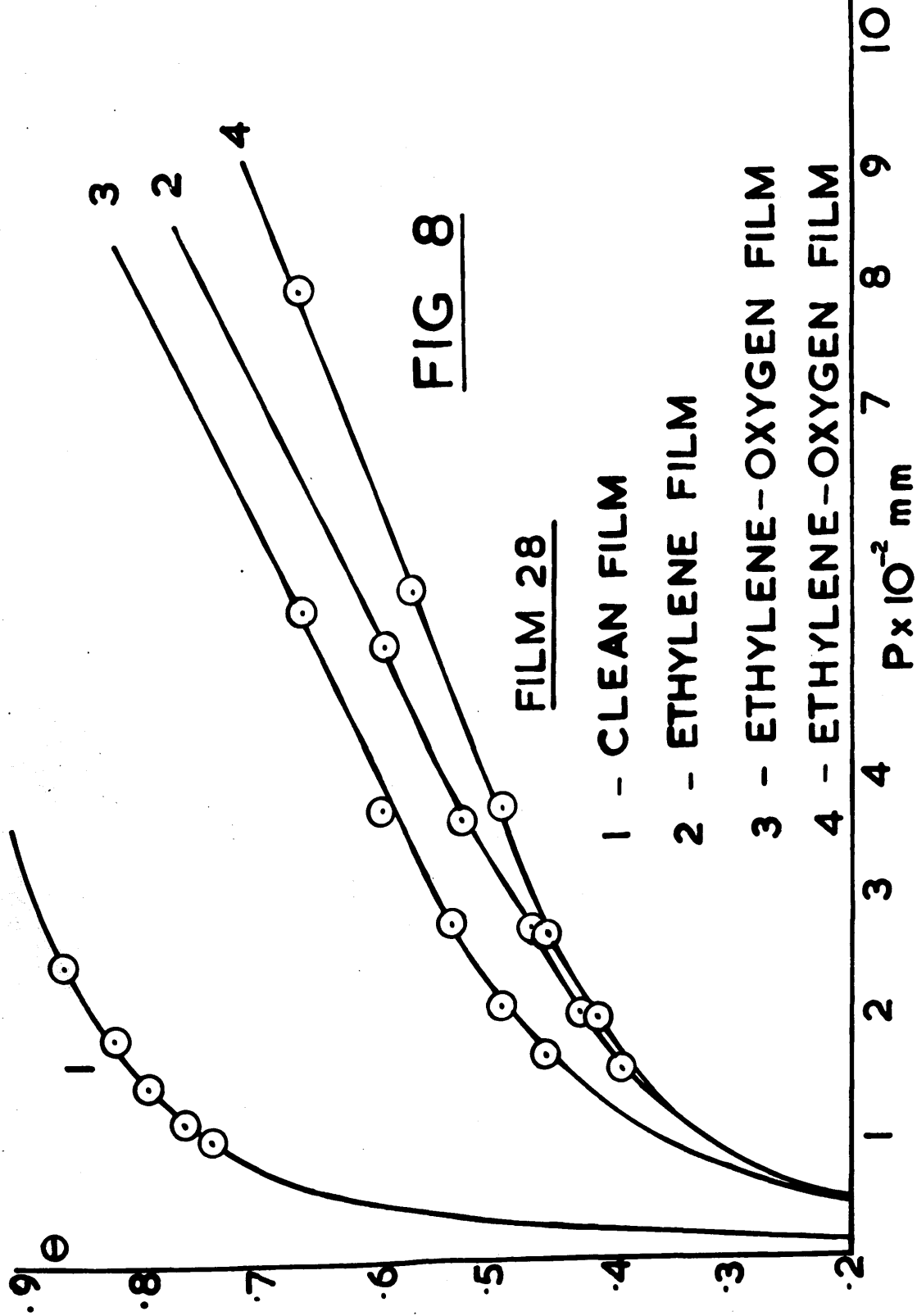
FILM 27

1 - CLEAN FILM

2 - ETHYLENE FILM

3 - ETHYLENE OXYGEN FILM





Figs. 6, 7 and 8 are the coverage curves obtained for those films which had ethylene and oxygen adsorbed on them. The coverages for these films were based on the  $V_m$  value for the clean surface. It can be seen that for the chemisorbed surfaces the coverage is lower than that on a clean film at any given pressure, which supports the idea that there is greater lateral repulsion between the krypton atoms.

## CHAPTER IV

Surface area determinations of nickel  
films which have adsorbed mercury or caesium

## CHAPTER IV

### Surface area determinations of nickel films which have adsorbed mercury or caesium

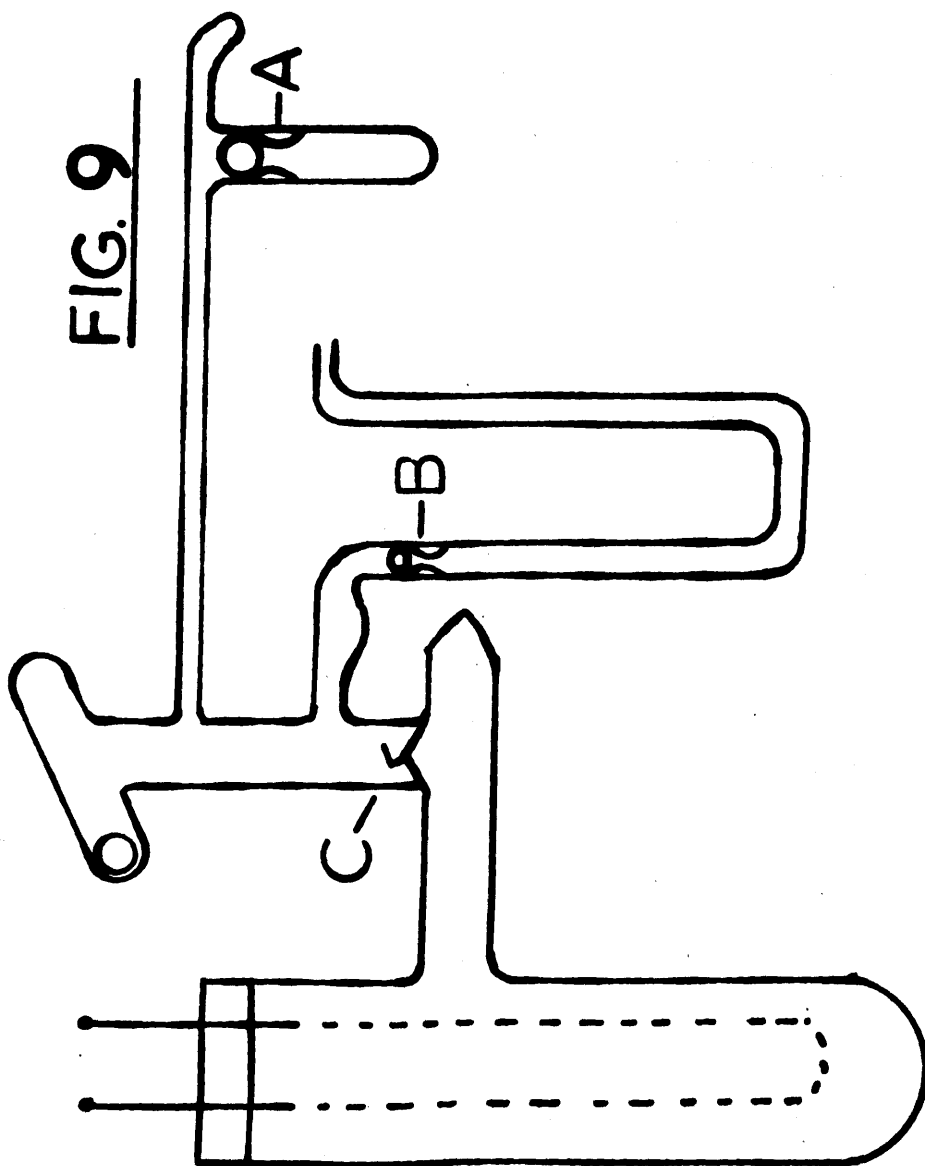
#### Part I

#### Nickel Mercury surfaces

##### 4.1 Introduction

It has been shown experimentally that a chemisorbed species, adsorbed on a high vacuum evaporated nickel film, in some way changes the volume of krypton required to form a monolayer on the surface. In addition to the factors previously discussed the relationship between the amount of the species chemisorbed and the resulting change in  $V_m$  should help to establish how this change in  $V_m$  arises. It was decided therefore to investigate this relationship using radio-mercury as the species to be chemisorbed. Radio-mercury was chosen since it could be adsorbed in carefully controlled quantities, and since the total amount of mercury adsorbed at any given time could be measured by a simple counting technique.





## 4.2 Experimental

### Apparatus

The apparatus was the same as for other experiments, except for some simple modifications to the catalyst vessel and protecting U-tube as shown in Fig. 9. The side arm and finger containing the radio-mercury was fitted with a ground glass seal A and steel ball. This was to reduce diffusion of radio mercury onto the nickel surface while the mercury already adsorbed on this surface was being counted. The protecting U-tube was also fitted with a ground glass seal B and steel ball to reduce distillation of the radio-mercury into this U-tube. This was necessary, since if radio-mercury were to distil into the protecting U-tube it would interfere with the count rate obtained for the mercury adsorbed on the nickel surface.

## 4.3 Experimental Procedure

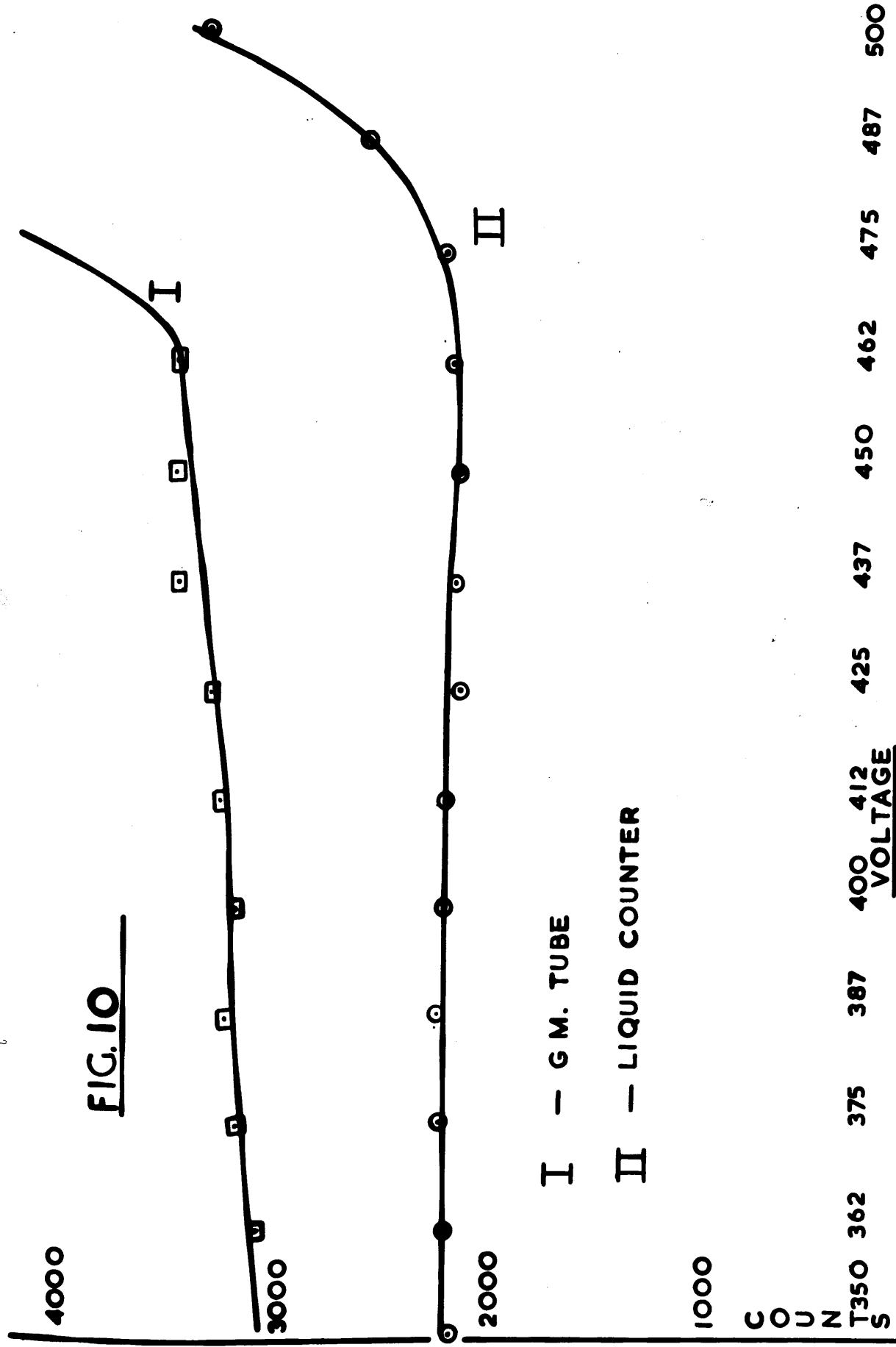
The catalyst vessel and U-tube were immersed in a large flask of liquid nitrogen. The finger containing the radio-mercury was immersed in liquid nitrogen in a separate flask. The break seal C was

broken and the surface area of the clean film determined in the usual manner. The large flask of liquid nitrogen surrounding the catalyst vessel and U-tube was removed and a smaller flask of liquid nitrogen quickly placed round the U-tube only. The krypton used in the surface area determination was then pumped away. A magnet was used to lift the steel balls on or off their valve seatings. Both valves were kept closed, except when the following operations required krypton or mercury vapour to be allowed to pass through them. Mercury was allowed to diffuse onto the nickel film. The mercury in the finger was then shielded with a lead container and the mercury on the <sup>nickel</sup> surface counted. The lead shielding was removed and the mercury finger immersed in liquid nitrogen. The small flask of liquid nitrogen surrounding the U-tube was removed, and the catalyst vessel and U-tube once more immersed in the large flask of liquid nitrogen, and the surface area re-determined. The process was repeated until sufficient measurements had been made to enable a graph of surface area vs. weight of mercury adsorbed to be drawn.

#### 4.4 Direct counting of mercury adsorbed on film surface

A Mullard type MX120 G.M. tube was used to measure the activity of the mercury on the nickel film. Fig. 10 shows the characteristic plateau obtained for this tube. The counter was connected via an Ericsson Telephones Ltd., type 110A probe unit to an Ekco. scaler, type No. N5298, on which the counts were recorded. In order that maximum counting efficiency be obtained it was necessary to place the G.M. tube in contact with as much of the catalyst vessel as possible. It was found that the count rate obtained was extremely sensitive to the relative positions of the counter and catalyst vessel. A glass container was designed for the counter and this could be clamped in the same position relative to the catalyst vessel for different counts. This ensured that the count rates, obtained at different times, were reproducible. Comparing count rates at different times gave a measure of the relative amounts of mercury present. These amounts could be calculated in absolute units by the procedure described in the next section.

**FIG. 10**



#### 4.5 Calculation of amount of mercury adsorbed.

After the last surface area determination had been done the nickel film was dissolved in 25 ml. of 10N nitric acid and a sample of the solution counted in a liquid counter. A standard solution of mercury of the same specific activity was made up in 10N nitric acid, and this solution was also counted in the same liquid counter. Since the count rate is proportional to the weight of mercury, the total weight of mercury adsorbed by the film could be calculated. This weight of mercury corresponded to the final count rate obtained for the surface using the G.M. tube, and so by proportion the weights of mercury corresponding to the other surface counts could be obtained.

#### 4.6 Counting of Radioactive Solutions

10 ml samples of the mercury solutions were counted successively in the same counter. This was a liquid counter type M64 supplied by Twentieth Century Electronics and was connected to a probe unit and scaler of the type mentioned previously (section 4.4). Fig. 10 shows the characteristic counting plateau obtained with this counter.

#### 4.7 Results and discussion of films which have adsorbed mercury

The first ionisation potential of mercury is 10.43 volts whereas the work function of nickel is only 5.03 volts, it would seem therefore that when mercury is adsorbed by a nickel surface it will accept rather than donate an electron. Consequently the mercury will tend to carry a net negative charge, which would tend to polarise subsequently adsorbed krypton atoms to a greater extent than the clean surface. As has been inferred in Chapter III this would lead to increased lateral repulsion between the krypton atoms and consequently a decrease in the value of  $V_m$ .

As can be seen from table 13 adsorption of mercury causes a decrease in the volume of krypton which will subsequently <sup>be</sup> adsorbed. This decrease in the volume of krypton adsorbed is proportional to the amount of mercury adsorbed. Table 14 shows that a point is reached when further adsorption of mercury no longer causes a decrease in the volume of krypton adsorbed. The maximum decrease observed was of the

TABLE 13Film 45

$V_m$ cm <sup>3</sup> mm at 300°K	Wt. of Mercury adsorbed in mg.	Atoms of mercury adsorbed $\times 10^{16}$
136.0	0.000	0.000
135.0	0.090	0.268
126.0	0.591	1.765
118.0	1.143	3.418
106.0	1.667	4.460
96.3	2.252	6.720
68	3.981	11.900
39.5	7.499	22.350
33.2	10.006	29.800

Film weight = 36.99 mg.



**TABLE 14**

**Film 42**

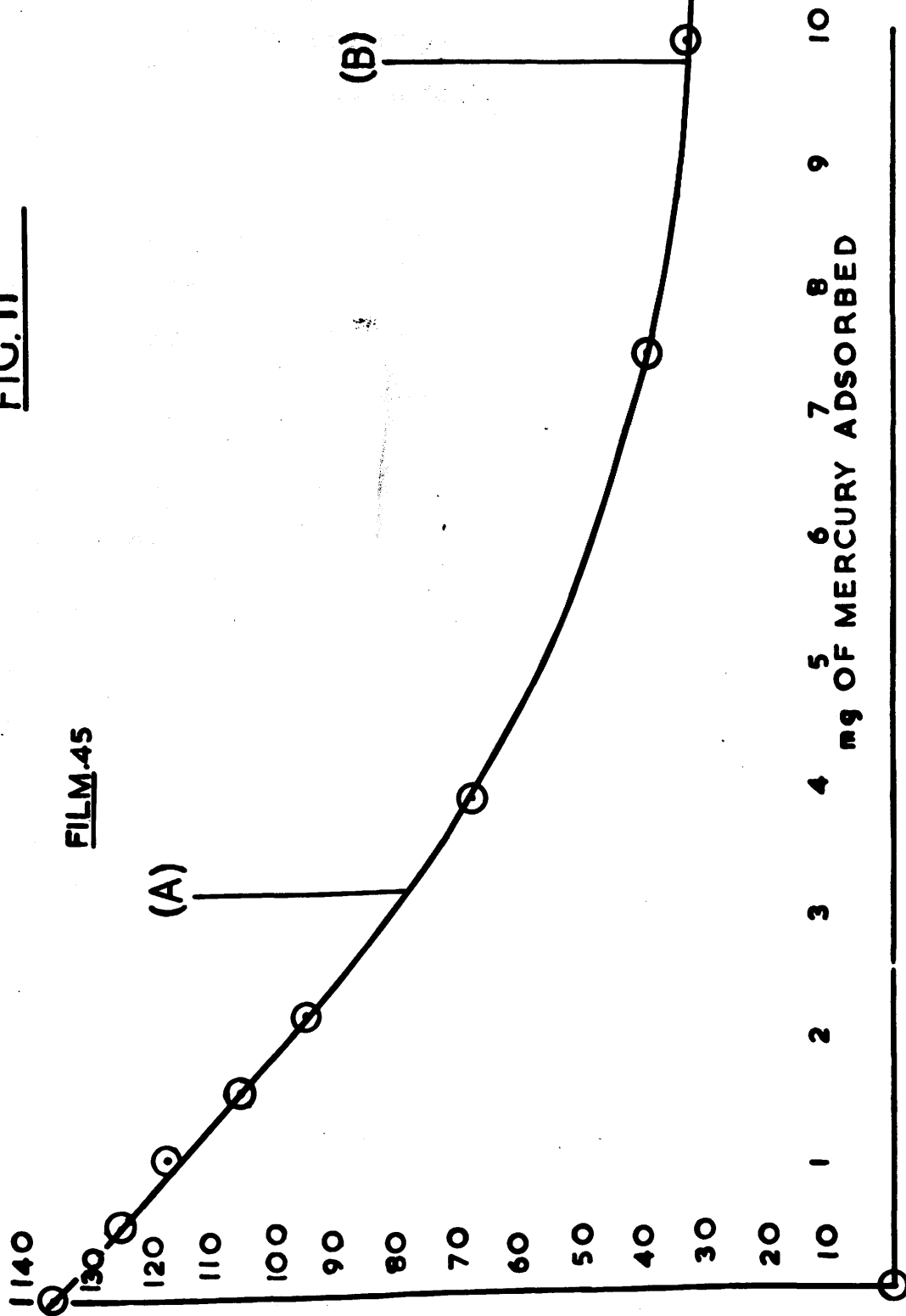
$V_m$ cm <sup>3</sup> mm at 300°K	Weight of Mercury adsorbed mg.
49.0	0.000
24.3	4.369
24.3	11.151
24.3	14.952
24.3	23.133

order of 80%. Fig. 11 shows the results of table 13 in the form of a graph of  $V_m$  plotted against weight of mercury adsorbed. This curve consists of a linear portion and a smooth curve which seems to straighten out into another linear portion.

Fig. 11 shows that the volume of krypton required to form a monolayer on the surface,  $V_m$ , falls linearly as the amount of mercury adsorbed increases. This continued until point A on the curve was reached. The point A corresponded to the completion of a monolayer of adsorbed mercury. This coverage was based on the amount of hydrogen which the film would have adsorbed, and on the assumption that this hydrogen would have covered 70% of all the available nickel sites. At point A the slope of the line changed and the linear portion became a smooth curve. This then showed that further adsorption of mercury after a monolayer has been formed had much less effect on  $V_m$ . This more gradual decrease in  $V_m$  continued as increasing amounts of mercury were adsorbed until the point B was reached. This point B corresponded to the formation of three

VMCC/mm.

FIG. II



monolayers of mercury on the nickel surface.

Further adsorption of mercury beyond this point seemed to have very little effect on the value of  $V_m$ .

The results of the mercury adsorption experiments have a bearing on the question of the adequacy of the cooled U-tube as a method of protecting the nickel surface from mercury contamination, and so this problem is discussed in the next section.

#### 4.8 Mercury Contamination as a source of error in surface area determinations.

In normal experimental procedure the catalyst vessel was at all times protected by a U-tube immersed in liquid nitrogen, except for the few seconds when one flask of liquid nitrogen was being replaced by another. This time interval was so short that the temperature of the protecting U-tube never rose appreciably above  $-195^{\circ}\text{C}$ . As can be seen from table 15 the amount of mercury which had adsorbed after a period of ten minutes at  $20^{\circ}\text{C}$  was very small, and had a negligible effect on the surface area of the nickel film. Even after a period of thirty minutes, for the last ten of which the mercury source was at a temperature of  $45^{\circ}\text{C}$ , the decrease in  $V_m$  caused by

TABLE 15

Vm in cc/mm at 300°K	Weight of Mercury adsorbed mg.	Time of Exposure	Temperature of mercury source
136.0	0.000	0.000	-
135.0	0.090	10 minutes	20°C
126.0	0.591	<del>10 minutes</del> + 10 minutes	20°C 45°C

this mercury was only about 7%. It can be seen then that mercury contamination of clean films, protected at all times by a U-tube kept at  $-195^{\circ}\text{C}$ , will be negligible.

## PART II

### 4.9 Introduction to Caesium adsorption Experiments

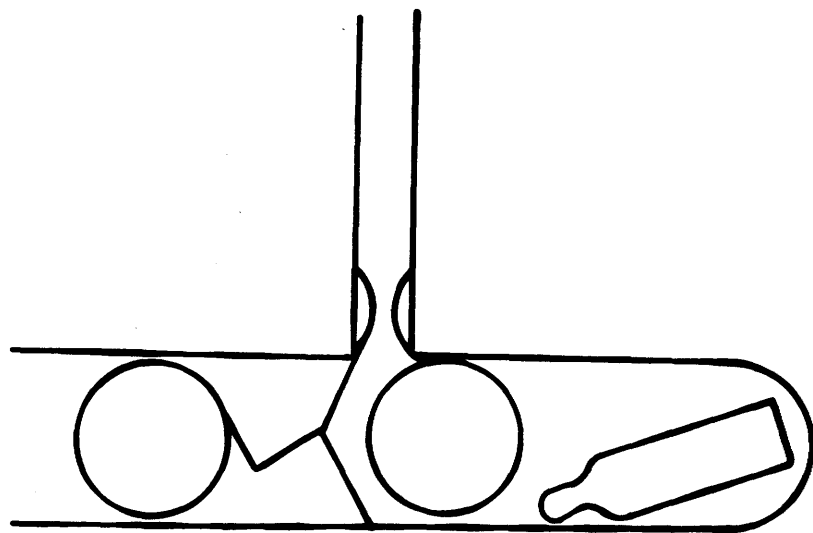
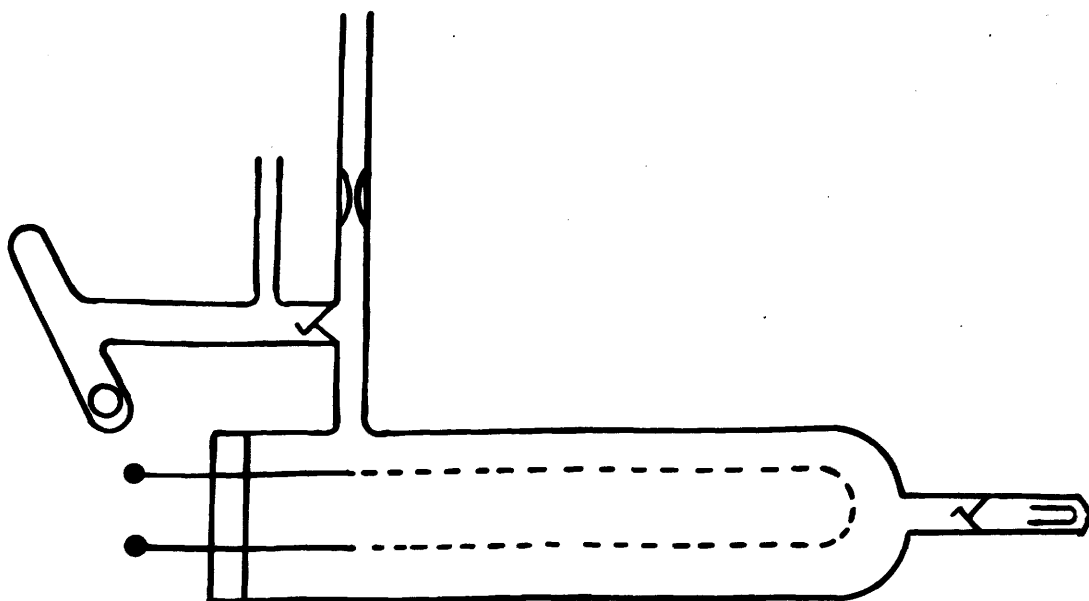
It has been shown that both positively and **charged** negatively adsorbed layers on a nickel surface might be expected to cause a decrease in the value of  $V_m$ . This decrease in  $V_m$  has been attributed to enhanced polarisation of the krypton atoms in the first adsorbed layer. The only positively adsorbed film so far studied was an ethylene adsorbed nickel surface. Since there was some doubt as to the relative coverage of a nickel film with ethylene, it was decided to investigate the effect of some other adsorbate which would <sup>be</sup> adsorbed with a positive dipole and a high relative coverage of the nickel surface to confirm that the decrease in  $V_m$ , due to increased lateral repulsion, was independent of the sign of the induced dipole.

An element will only donate an electron to the nickel when it is adsorbed, if its ionisation potential is less than the work function of the nickel. As the work function of the nickel is 5.03V the choice of adsorbate is restricted to the metals of Groups I and II of the Periodic Table. The ideal adsorbate would therefore be caesium which has the lowest ionisation potential of all the elements, being only 3.89V. Another factor in the favour of the use of caesium as adsorbate, is that for a metal it has a high vapour pressure. It was thought then, that sufficient caesium would <sup>be</sup> adsorbed on the nickel, without the caesium having to be heated to such a high temperature as to lead to the possibility of thermal sintering effects in the nickel film.

#### 4.10 Experimental

In designing catalyst vessels for these experiments it was of prime importance that the metallic caesium be as close as possible to the nickel film, in order to avoid undue condensation of the caesium on the glass walls when being distilled onto the nickel surface. The most successful design, the one used for these experiments, is shown in Fig. 12.

FIG. 12





The caesium, which was 99.999% pure, was obtained from L.Light and Co. in 0.5 gm. samples sealed in glass ampoules. Great difficulty was experienced in transferring this caesium to the catalyst vessel, since the caesium would react violently if allowed to come into contact with the atmosphere. This problem was overcome as follows: The ampoule was scratched all the way round the neck with a glass knife, and then placed with a steel ball in a tube fitted with a break seal and side arm containing a constriction. The bottom of this tube was then sealed and rounded off. The side arm was sealed to the vacuum system and evacuated. Using a powerful magnet, the steel ball was used to break the ampoule at the neck, where it had been scratched. After further evacuation the tube was sealed off at the constriction, a steel ball carefully placed on top of the break seal, which was then joined to the catalyst vessel. This tube containing the caesium is shown in Fig. 12.

#### 4.11 Experimental Procedure

After the catalyst vessel had been joined to the adsorption apparatus, and the system evacuated,

the surface area of the clean film was determined in the usual manner. The large flask of liquid nitrogen was then removed from around the catalyst vessel and U-tube, and the U-tube immediately immersed in a flask of liquid nitrogen, to avoid contamination of the surface with mercury. The break seal on the finger containing the caesium was broken and some caesium allowed to distil onto the surface of the nickel film. The distillation of the caesium was effected by immersing the finger in hot water or by heating gently with a soft flame. The latter method was used to distil on the last sample of caesium. The large flask of liquid nitrogen was then replaced round the catalyst vessel and U-tube and the surface area redetermined, correction being made for the increased volume of the system. The surface area determinations were repeated for subsequent samples of caesium adsorbed on the surface.

#### 4.12 Results and discussion of caesium adsorption experiments

It was postulated that adsorption of caesium as a positive ion would cause enhanced polarisation of subsequently adsorbed krypton atoms, and as indicated in 3.2 this would lead to a decrease in the value of

$V_m$ . As can be seen from table 16 the experimental evidence substantiates this postulate. Although the results in table 16 indicate that the decrease in  $V_m$  was proportional to the amount of caesium adsorbed, it was impossible to equate the decrease in  $V_m$  with the fraction of the surface covered with caesium due to the fact that the amount of caesium adsorbed could not be measured. The last sample of caesium was distilled on to the nickel surface by heating the finger, in which the caesium was contained, with a soft flame, and as can be seen from table 16 this caused a 42% reduction in  $V_m$ .

Although the results in table 16 are as postulated by the dipole theory, since both the adsorbate and adsorbent are metals, and since the adsorbed caesium is non-localised the nature of the adsorbed caesium must be examined more closely. It is therefore relevant to consider such processes as the formation of a solid solution, and diffusion of the caesium into the nickel. As the atomic radius of caesium is about  $2.72 \text{ \AA}$  and that of nickel is about  $1.25 \text{ \AA}$  the formation of a solid solution is unlikely, since this is normally only permissible if the difference in the radii of the two metals is less than 15%.<sup>88</sup>

TABLE 16

Caesium Adsorption Experiments

$\text{cm}^3 \text{ VM}$ mm at $300^\circ \text{K}$	Description of Surface	Time of Exposure MINUTES	Temperature of Caesium
77.5	clean	0	-
63.6	adsorbed caesium	10	$40^\circ \text{C}$
61.5	adsorbed caesium	10	$40^\circ \text{C}$
45.0	adsorbed caesium	*	*

\* Caesium distilled onto nickel surface

When caesium is adsorbed by a nickel surface it does **forms** a positive ion, donating a 6s electron to the nickel. The adsorbed caesium is not localised on the surface, as in the case of adsorbed oxygen, and therefore the possibility of diffusion into the first or second layer of the nickel must be considered. Unfortunately no values for the diffusion coefficient of caesium on nickel are available. However, Langmuir and Taylor<sup>89,90</sup> have investigated the adsorption of caesium on tungsten: table 17 summarises their results. It is evident that even at 27°C the penetration of the caesium into the tungsten is of the order of 100 atomic layers in one second. It is inferred that similar diffusion takes place on nickel, so that even at 27°C, and neglecting any effect the heat of adsorption has, diffusion of the caesium would appear to be of importance.

Owing to the rapid diffusion of caesium into the nickel, it might be thought that this would result in the majority of the caesium being incorporated into the bulk of the nickel. However owing to the high porosity of the film, and its extreme thinness

TABLE 17

Diffusion of Caesium in Tungsten

Temperature °C	D cm <sup>2</sup> /sec	Penetration in cm. after one second
27	$1.2 \times 10^{-11}$	$3.47 \times 10^{-6}$
227	$1.5 \times 10^{-7}$	$3.88 \times 10^{-4}$
427	$8 \times 10^{-6}$	$2.83 \times 10^{-3}$
540	$4 \times 10^{-5}$	$6.32 \times 10^{-3}$

(about 1000 Å), the ratio of surface nickel atoms to the total number of nickel atoms is relatively high, and therefore a large proportion of the caesium will remain on surface sites. It is therefore inferred that diffusion of the caesium does not necessarily invalidate the conclusions drawn from the results in table 16, that a positively adsorbed species causes enhanced polarisation of krypton atoms, resulting in the observed decrease in  $V_m$ .

It is evident from table 18 that adsorption of very small amounts of caesium caused an increase in the value of  $V_m$ . Although this increase was small (4%) the measurements were reproducible and hence the increase was assumed to be genuine. It was thought that a mechanism similar to that postulated in section 3.4 for the hydrogen covered films might explain this increase in the value of  $V_m$ .

In view of the surface mobility of the adsorbed caesium ions, and the ease with which they appear to diffuse in the nickel, it is conceivable that at very low coverages the adsorbed caesium would behave differently.

TABLE 18

Caesium adsorption experiments

$V_m \text{ cm}^3_{\text{mm}}$ at $300^\circ\text{K}$	Temperature of caesium	Time of Exposure mins.
56.8	-	0.0
57.2	$20^\circ\text{C}$	1
57.0	$20^\circ\text{C}$	1
57.7	$20^\circ\text{C}$	1
59.1	$20^\circ\text{C}$	1



The caesium ions would tend to delocalise the electrical double layer present at the nickel surface, consequently subsequent adsorption of krypton atoms would still be on a nickel surface, but on a nickel surface which has an attenuated electric field. This would result in less polarisation of the krypton atoms and hence decrease lateral repulsion. As has been explained before this would lead to an increase in  $V_m$ .

## CHAPTER V

### Gas Adsorption Apparatus

## CHAPTER V

### Gas Adsorption Apparatus

#### 5.1 McLeod Gauges

Since it was necessary to measure the pressure of the adsorbed gases with high accuracy a McLeod gauge was chosen for this purpose. This gauge had the advantages of simplicity of construction and of being independent of the presence of mercury vapour. Again since the same gauge could be used for all pressure measurements, any systematic errors in the absolute measurement of pressure would be common to all measurements and the overall experimental error would thus be reduced. Since the function of the gauge depends on the application of Boyle's Law and since the deviation of the gases used from Boyle's Law at low pressure are slight, further justification for employing a McLeod gauge was provided.

It was thought that these advantages outweighed the fact that mercury vapour is a catalyst poison and so is capable of being adsorbed by the film. Other pressure measuring devices such as ionisation gauges, Penning gauges,

and Piranigauges were not sufficiently accurate and suffered the disadvantage that they have to be frequently calibrated. They suffer the added disadvantage in that they do not give consistent readings for different gases at the same pressure.

The size and compression ratio of the gauges were determined by the maximum and minimum pressures of gases to be used in the experiments, taking into account the volumes of the associated sections, and the need to ensure adequate amplification of the lowest pressures to a value that could be read accurately by the instrument.

As mentioned before, measurement of pressure on a McLeod gauge depends on the application of Boyle's Law. If the volume in  $\text{cm}^3$  of the gas trapped in the gauge at unknown pressure  $p_{\text{cms}}$  is  $M$ , and if  $A\text{cm}^2$  is the capillary cross sectional area, and  $h$  the difference in height between the mercury columns in the closed and comparison limbs, then Boyle's Law gives

$$p(V_0 - hA) = Ah \times h$$
$$\text{i.e. } p = Ah^2/M - Ah = Ah^2$$

since the volume of the capillary is small compared with M.

This formula assumes that the meniscus in the comparison tube is raised to the same level as the end of the capillary in the closed limb each time. If this is not done, the formula becomes

$$p = A(h_1 \times h_2)/M$$

where  $h_1$  is the distance between the end of the capillary in the closed limb and the meniscus in that limb, and  $h_2$  is the difference in heights of the menisci. Factors influencing the reliability of McLeod gauge measurements are the accuracy with which  $h_1$  and  $h_2$  can be determined, and also the accuracy of the M calibration.

Discrepancies in measuring true values of  $h_1$  and  $h_2$  arise because of capillary depression.<sup>91</sup> Porter<sup>92</sup> showed that the discrepancies increased with decreasing capillary diameter, and were caused by the variation of the angle of contact between the mercury and the glass. This angle could vary between  $30^\circ$  and  $60^\circ$  in a gauge in which the mercury and the glass were apparently perfectly clean. Rosenberg<sup>93</sup> and Klemperer<sup>94</sup> showed that roughening the inside of the capillaries,

for example by using a mild abrasive such as alumina considerably reduced the error.

Further causes<sup>96</sup> are slight oxidation of the mercury after exposure to air and the state of cleanliness of the inside surface of the tubes, error being caused, for instance, by the presence of adsorbed water vapour. It is then of the utmost importance to ensure that the glass and mercury are initially perfectly clean and to allow air to come in contact with the interior of the gauge as seldom as possible once it had been evacuated and degassed.

Figures quoted<sup>97</sup> for the errors to be expected from carefully constructed McLeod gauges show that the error due to capillary depression becomes increasingly important at pressures below  $10^{-4}$  mm, at which pressure it is of the order of  $\pm 2\%$  and very much higher at lower pressures.

The capillaries in the gauge used were constructed from 0.15 cm diameter tubing, this being considered a suitable compromise, bearing in mind the increasing

error incurred with narrow bores and the need to make  $h_1$  and  $h_2$  as large as possible to reduce errors in their measurement. It was decided to employ Veridia Precision Bore tubing supplied by Chance Brothers Ltd., Birmingham, which has a tolerance of  $\pm 0.01$  mm. in bore diameter and a low coefficient of expansion. Another advantage of this product is that, because of the manufacturing method of collapsing the glass on to a mandrel of precision diameter which is then dissolved away, the bore is left with a somewhat translucent, roughened finish and is therefore, ideal for the construction of McLeod gauges to Rosenberg's recommendation.

## 5.2 Construction of McLeod gauges

The closed limb of the gauge was made of 0.15 cm. precision bore tubing, the closed end being formed by rotating the tube in a soft oxygen blow pipe flame. Care was taken to heat as short a length of the tubing as possible, since high temperature caused the etched appearance of the glass to disappear. The end of capillary assumed a perfectly hemispherical shape. The tube was cleaned thoroughly with chromic acid solution and washed with water. The final washing was

done with distilled water.

The closed limb was then fused to a bulb which had a B24 cone and dip tube for fitting to the quickfit conical flask which was to contain trebly distilled mercury. To increase the accuracy of the gauge the entry to the bulb was constricted by a 2 cm length of 0.5 cm. diameter tubing fitted by a ring seal to the bottom of the bulb. The side arm containing the reference limb, made from the same length of tubing as the closed limb, was joined immediately below this seal fig. 13. Before calibration the entire gauge was cleaned in the manner of the closed limb.

It has been shown by Cranstoun<sup>98</sup> that the precision bore tubing used in the construction of the McLeod gauges has a very high degree of linearity and constancy.

Before use, the gauge was evacuated for several days and checked for reproducibility. The calibration of the gauges is shown in appendix B.



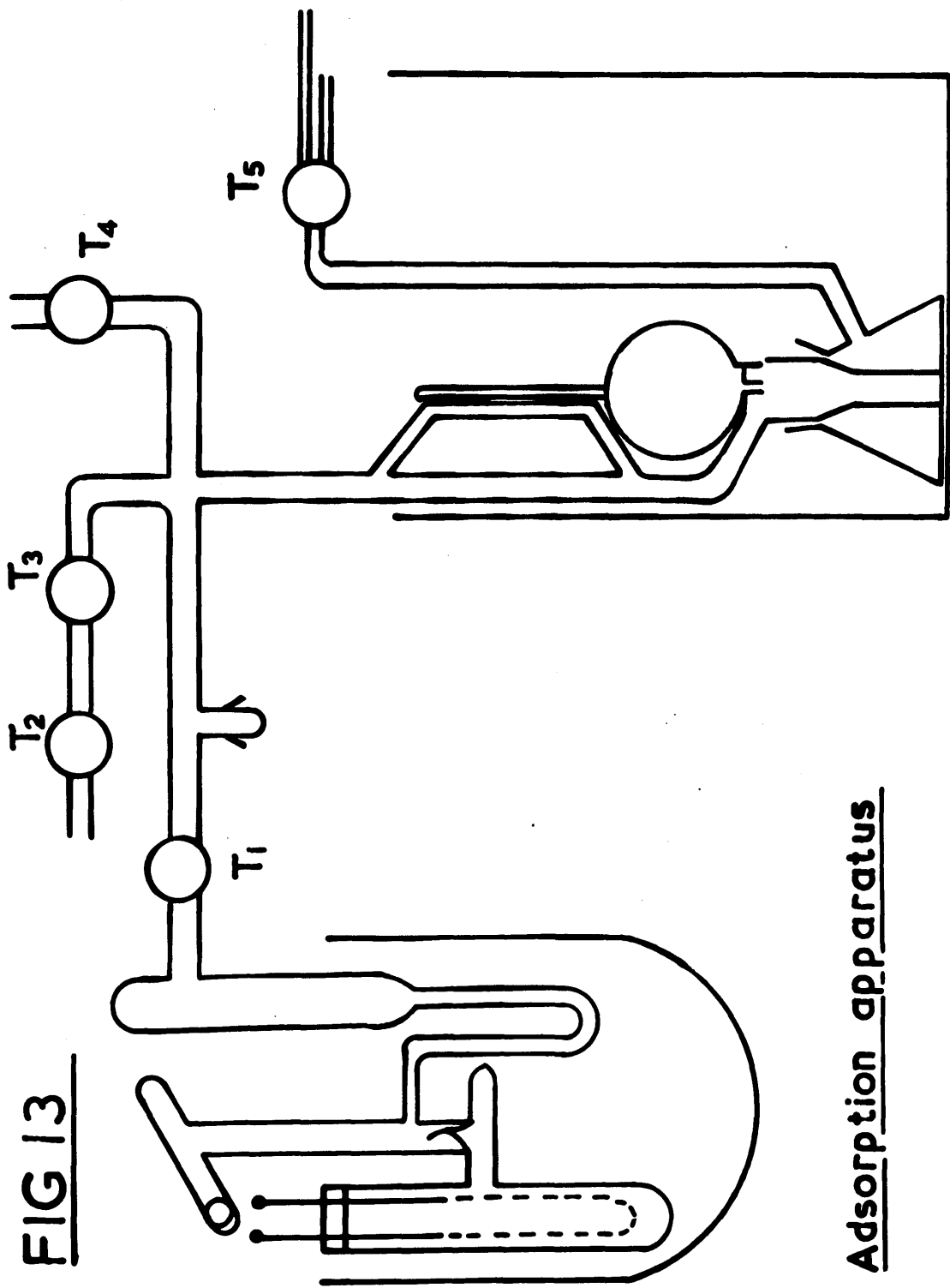


FIG 13

Adsorption apparatus

### 5.3 Gas Adsorption Apparatus

This primarily consisted of a catalyst vessel a gas pipette and a McLeod gauge, Fig. 13. The construction of the catalyst vessel and McLeod gauge are described elsewhere. The U-tube protecting the catalyst vessel from mercury contamination was made from Pyrex glass of internal diameter 0.6 cm. This was connected to a length of wider bore tubing 1.3 cm. internal diameter. It was this tubing which was in the temperature gradient. This wider tubing was used as this decreased thermal transpiration. Taps  $T_1$  and  $T_2$  were 6 mm in internal diameter the connecting tubing was Pyrex of internal diameter 0.8 cm. Taps  $T_2$  and  $T_3$  were 4 mm. and the connecting tubing was 0.7 cm. internal diameter. The tubing to the McLeod gauge was 0.7 cm. internal diameter and the two way tap  $T_5$  was 2 mm. A B.14 socket was fused to the tubing between tap  $T_1$  and the McLeod gauge. This provided a method of attaching a second McLeod gauge so that measurement could be made in a different pressure range. It also provided a point for attaching additional gas reservoirs where freshly prepared samples could be stored.

The catalyst vessel the U-tube and associated tubing to tap  $T_1$  was called volume C and was calibrated for each experiment by expansion of helium. The volume between tap  $T_1$  and  $T_4$  excluding the volume of the McLeod gauge bulb and capillary was volume D and was  $85 \text{ cm}^3$ . The volume of the McLeod gauge bulb was  $137.9 \text{ cm}^3$  and the volume of the gas pipette between taps  $T_2$  and  $T_3$  was  $4.775 \text{ cm}^3$ .

#### 5.4 Operation of Gas Adsorption Apparatus for surface area Determinations.

Taps  $T_1$  and  $T_2$  were opened and the system evacuated until a vacuum of better than  $10^{-6}$  mm of mercury was obtained, as measured on the most sensitive McLeod gauge. Taps  $T_1$  and  $T_2$  were then closed and a sample of krypton admitted using the dead space between taps  $T_2$  and  $T_3$  as a gas pipette. The pressure was measured and tap  $T_1$  opened. The catalyst vessel and U-tube were then immersed in a vacuum flask containing liquid nitrogen and the break seal on the catalyst vessel broken. About twenty minutes was allowed for the krypton in the adsorbed and gaseous state to reach equilibrium.

The pressure was then measured. Tap  $T_1$  was closed and  $T_4$  opened and the McLeod gauge and associated dead space evacuated. Tap  $T_4$  was then closed and  $T_1$  again opened and the pressure measured after another period of fifteen minutes. This procedure was repeated until sufficient readings had been obtained to plot the B.E.T. graph.

### 5.5 Chemisorption of gases

A sample of the gas to be chemisorbed was admitted to the calibrated volumes C and D using the dead space between taps  $T_2$  and  $T_3$  as a gas pipette. The pressure was measured and  $T_1$  opened and the gas allowed to be chemisorbed by the catalyst surface. This procedure was repeated until the desired amount of gas had been adsorbed.

The method of estimating the amount of nitrous oxide which had decomposed was complicated by the fact that, as the nitrous oxide decomposed on the catalyst surface, gaseous nitrogen was produced. The method of measurement was as follows. A sample of nitrous oxide was admitted to the system and allowed to decompose. The U-tube was then immersed in liquid nitrogen. If there was no decrease in pressure this

meant that all the nitrous oxide had decomposed.

The liberated nitrogen was pumped off and the process repeated until there was a decrease in pressure when the U-tube was immersed in liquid nitrogen.

The pressure of the nitrogen in the gas phase was then measured and this was proportional to the amount of nitrous oxide decomposed in the last sample. The total amount decomposed was obtained by adding this to the samples previously added.

#### 5.6 Protection of the catalyst from Mercury Vapour

It is well established that mercury is a catalyst poison. Not only does it prevent chemisorption of many gases such as hydrogen, it also in some way affects the physical adsorption of krypton. As the results in section 4.7 show adsorbed mercury causes significant changes in the volume of krypton required to form a monolayer on the surface. Accordingly precautions had to be taken to ensure that at no time did mercury vapour come in contact with the catalyst surface. This was accomplished by immersing the U-tube shown in Fig. 13 in liquid nitrogen. As the results in section 4.8 show this was effective in preventing mercury vapour from reaching the catalyst surface. A simple U-tube

was used in preference to a spiral trap, since experiment showed that the flow rate of gases through this was very slow, particularly at low pressures. This problem of slow diffusion was also experienced where stopcocks of narrow bore were used. Consequently where ever possible large-bore stopcocks were used, in particular Tap  $T_1$  in Fig. 13. This problem of diffusion of gases at low pressures is discussed by Partington.<sup>99</sup>

When easily condensable gases such as nitrous oxide and ethylene were present, it was necessary to substitute an acetone and solid carbon dioxide freezing mixture for the liquid nitrogen so that condensation of these gases did not take place.

## 5.7 Storage of gases

Since it was possible to prepare large quantities of the gases used and since the volume used per experiment was comparatively small, the question of storing gases for several months without risk of contamination was important. Bulbs sealed with greased vacuum taps were not suitable since after a time, the grease hardened, inducing streaking and subsequent leakage, both of the stored gas and air.

The need for regreasing such taps was frequent.

Accordingly it was decided to use mercury cut-offs. These had to be suitable for handling a large pressure differential of the order of an atmosphere and yet be suitable for the controlled issue of small amounts of gas. High pressure cut-offs have been described in the literature but these in general appear to be extremely complicated in structure. It was decided to design a simpler type which adequately fulfilled the required conditions. The cut-off is illustrated in Figs. 14, 15. The outer casing consisted of a Pyrex tube (1) 1.6 cm. in diameter and 80 cm. long, which had a B.24 cone at its lower end for fitting to a 250 ml. Quickfit mercury-containing round bottomed flask. A round bottomed flask was used as this has a less strained structure than a conical flask with a side arm. The mercury could be raised or lowered in the outer tube by connecting the flask to atmosphere or to the secondary vacuum line. This outer tube was connected to the adsorption part of the apparatus by means of a side arm which incorporated a ball valve to prevent the mercury flooding the vacuum system. Concentric with this outer tube, a second tube (2) 0.6 cm. in

FIG.14

Mercury cut-off

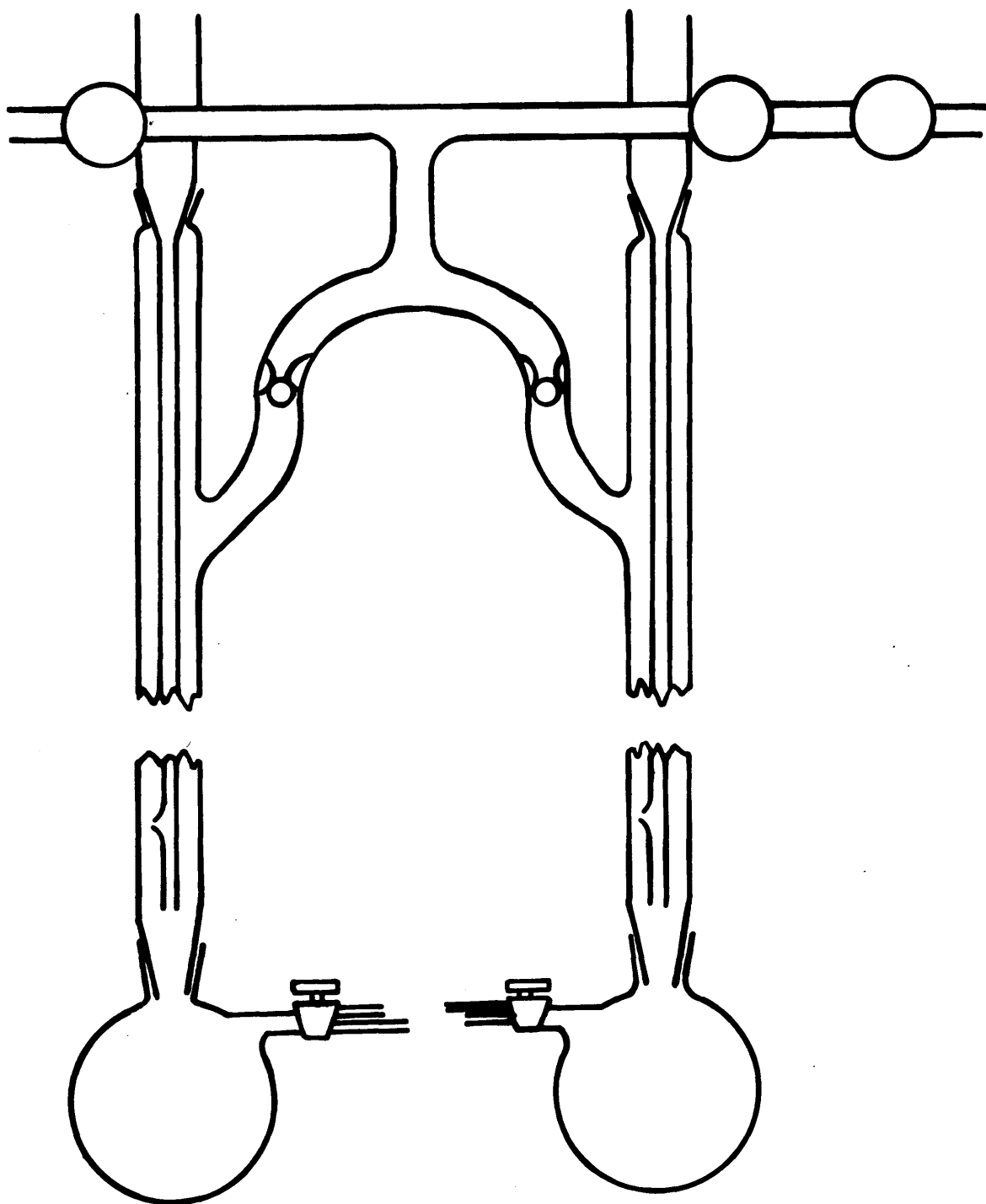
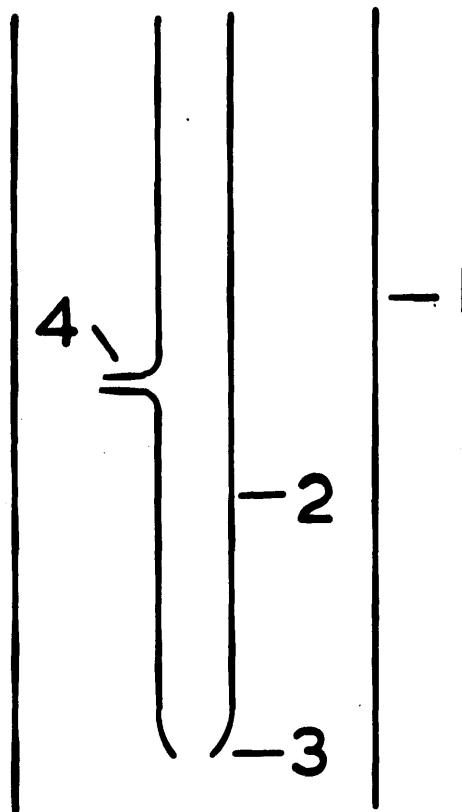




FIG 15



Mercury bubble valve.

diameter was connected to a 2-litre storage bulb via a B.14 cone and socket joint. The cone and socket was used instead of a ring seal, as this was less strained and made the apparatus easier to assemble. The bottom end of the tube (3), was left open to facilitate the filling of the storage bulb. About 10 cm. above the bottom of the inner tube was a fine nipple (4). This was made by softening the glass at this point touching with a glass rod and drawing out to a fine point. The end of this was broken off leaving a small hole about 0.5 mm. in diameter.

The method of operation was as follows:-

The mercury was lowered until the bottom of the inner tube (3), was above the level of the mercury, and the storage bulb evacuated. The storage bulb was then filled through the inner tube. When a satisfactory pressure of gas had been obtained the bulb could be isolated by connecting the round bottomed flask to atmosphere and the mercury level raised, cutting off the open end and nipple of the inner tube. When it was desired to withdraw gas from the storage bulb, the mercury was lowered slowly until the gas bubbled through the nipple through the outer tube and into the apparatus, via the side arm containing the ball

valve. This very fine nipple enabled small controlled amounts of gas to be withdrawn.

These cut-offs with their associated 2-litre storage bulbs were mounted in pairs, and were used to store nitrous oxide, hydrogen, oxygen and krypton.

### 5.8 The Purification of Hydrogen

The ability of palladium to adsorb hydrogen, specifically and in large quantities, is well known, and it was decided to make use of this property to purify hydrogen for adsorption purposes. In practice the hydrogen was allowed to diffuse through a heated palladium tube, and fig. 16 shows the apparatus used. The apparatus was essentially a water condenser with a B.19 socket at one end. Into this socket fitted a brass B.19 cone attached to a brass tube 17 cm. long with a palladium thimble silver soldered to the end of the tube. The palladium tube, which was supplied by Messrs. Johnson Matthey and Co. was thin walled 5 cm. long x 2.5 mm. outside diameter and closed at one end. The glass tube surrounding the palladium tube was heated electrically. It was insulated with asbestos paper and then wound with nichrome tape to a cold

**SECTION OF  
HYDROGEN  
PURIFICATION  
APPARATUS**

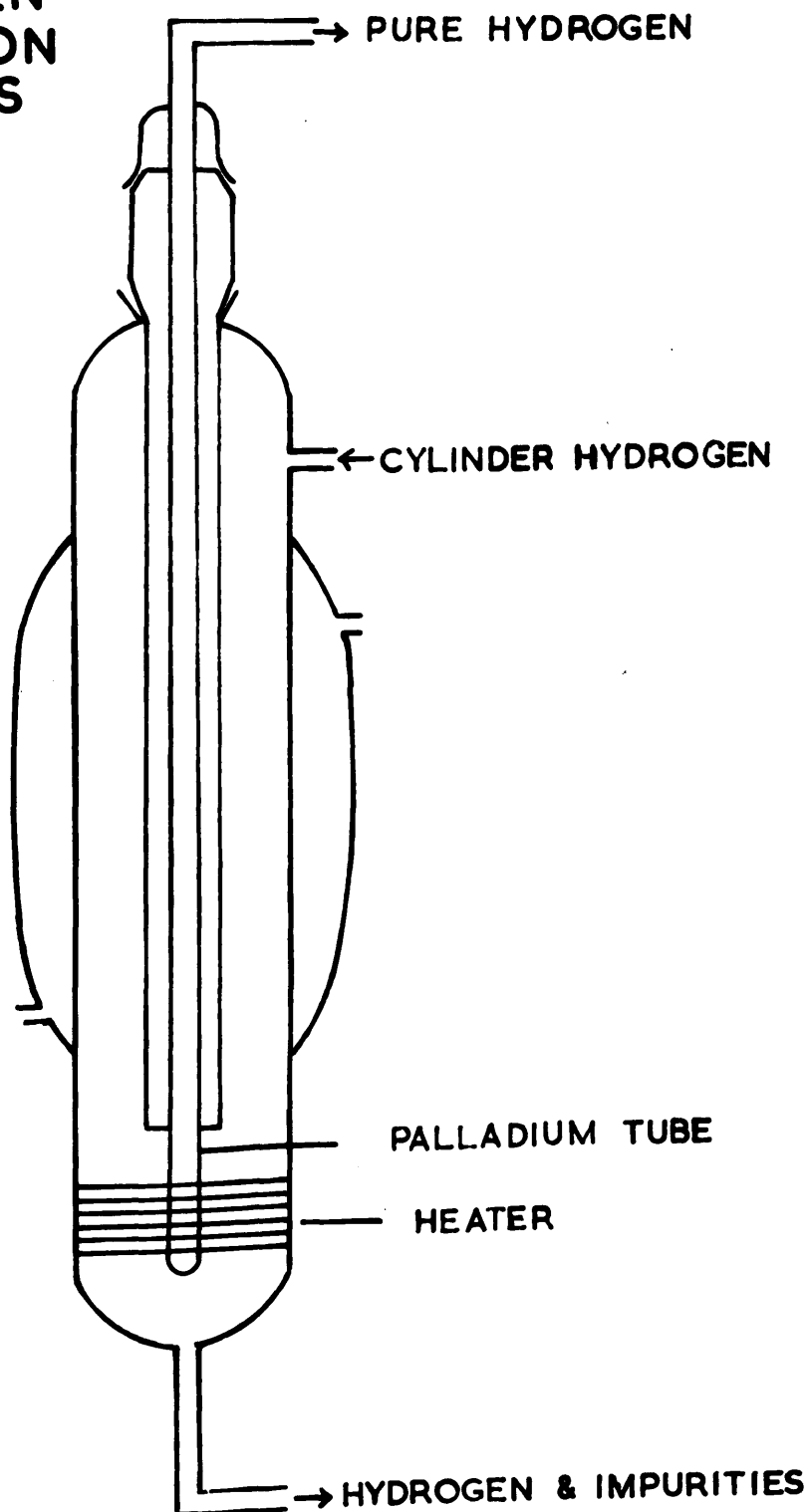


**FIG 16**

resistance of 35 ohms. The other end of the brass tube was connected via a Quickfit cone and socket to the gas storage section of the apparatus. Since brass is a very good conductor of heat it was essential that there was a rapid flow of cold water through the outer casing to avoid undue heating of this connecting joint, which was made vacuum tight with Apiezon wax.

#### 5.9 Preparation and purification of nitrous oxide and ethylene

These gases were supplied in cylinders by the British Oxygen Co. The gas was admitted to the system by connecting the cylinder to the apparatus via a mercury bubble valve. The gas was then condensed in a cold finger immersed in liquid nitrogen. The condensed gas was then pumped on to remove any permanent gas. It was allowed to warm up and the first fraction removed by connecting the cold finger to the pumping system. The gas was then condensed and again connected to the pumping system. The next fraction was allowed to expand into the storage bulb. The remaining gas was rejected.

#### 5.10 Oxygen, Krypton, Xenon, Helium

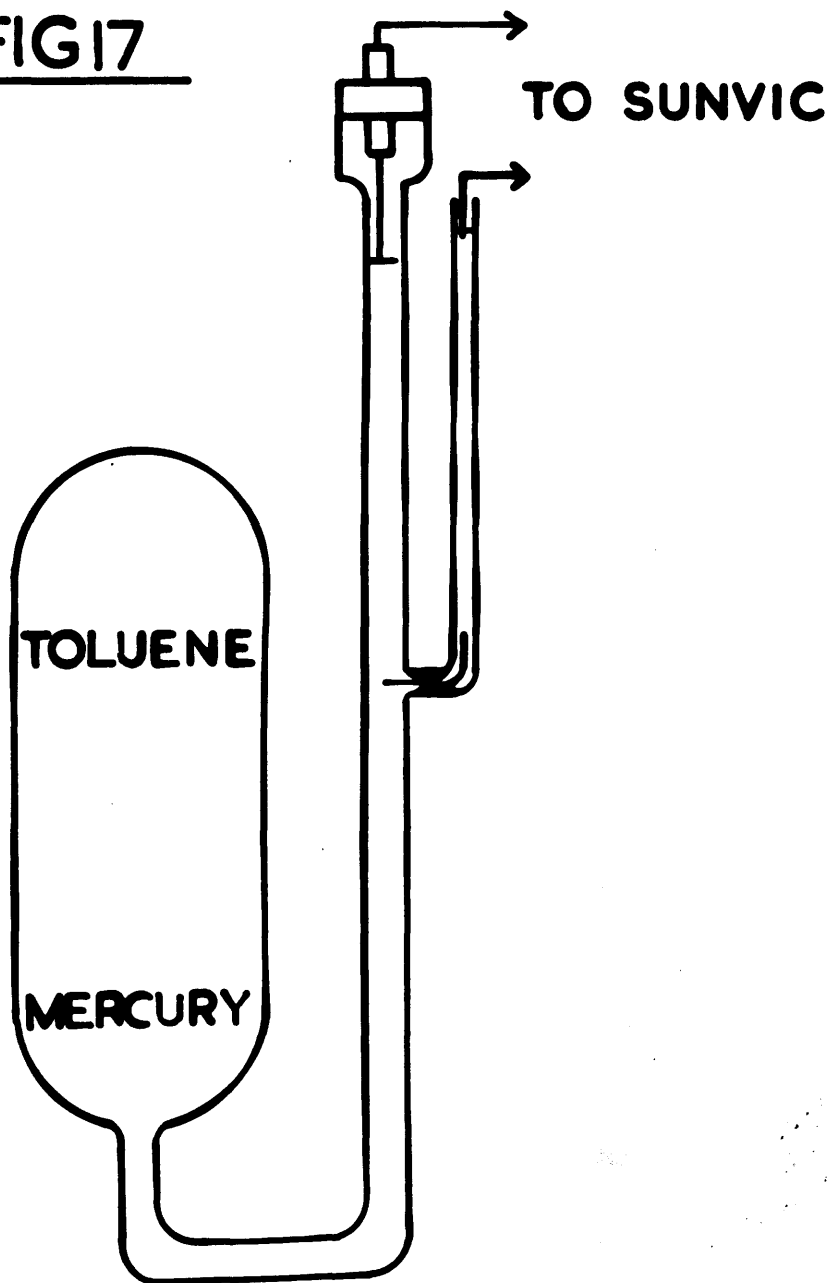
These gases were obtained from the British Oxygen Co. in 1-litre bulbs fitted with breakseals. The gases were spectroscopically pure. The krypton was not less than 99% pure, the remaining 1% being xenon. Similarly the xenon was 99% pure the balance being krypton.

#### 5.11 The Thermostat

As the temperature of the laboratory varied by as much as  $10^{\circ}\text{C}$ , and since this would affect the accuracy and reproducibility of pressure measurements, it was decided to thermostat the McLeod gauge. This was accomplished by immersing the gauge in a tank containing water at a constant temperature of  $300^{\circ}\text{K}$ .

The tank, which measured 46 cm. x 30 cm. x 30 cm., had an iron frame and glass windows. The window through which the McLeod gauge was read, was made of plate glass, specially selected for its uniformity of optical properties. The heater was a 250 watt Robertson flame lamp controlled by a Sunvic control unit and toluene regulator. Rapid circulation of the water was ensured by using a paddle type stirrer, driven by a 240 V Citenco motor. The Toluene regulator

FIG 17



Toluene Regulator

was made from a length of capillary tubing fused to a 12 cm. length of tubing 2 cm. in diameter sealed at one end as shown in Fig. 17.

A side arm was joined to the capillary and a piece of platinum wire pinch sealed at the join. The side arm was then filled with mercury to provide an electrical contact. An adjustable screw with a piece of platinum wire silver soldered to it, was attached to the capillary tubing and acted as the other electrical contact. The temperature of the tank was allowed to rise until  $300^{\circ}\text{K}$  had been reached. The screw contact was then adjusted until it just made contact with the surface of the mercury in the capillary tubing and so switch off the heater via the relay. When the temperature of the tank fell below  $300^{\circ}\text{K}$  the toluene contracted and the mercury level in the capillary tubing fell. This broke the circuit and the heating lamp switched on until the temperature had again reached  $300^{\circ}\text{K}$ . This system gave a mean temperature of  $300^{\circ}\text{K} \pm 0.05^{\circ}\text{K}$ .



Journal of Physical Chemistry

Vol. 61, No. 1, January 1957

## CHAPTER VI

### Preparation of Nickel films for Adsorption Studies

The preparation of nickel films for adsorption studies involves several steps. First, a clean, flat surface is required. This is achieved by etching a metal substrate, such as copper or silver, with a solution of ferric chloride and sulfuric acid. The etched surface is then rinsed thoroughly with distilled water and dried. A solution of nickel sulfate and nickel chloride is prepared, and a current is passed through it to deposit a thin layer of nickel on the etched surface. The deposition is controlled by the amount of current and the time of deposition. The resulting nickel film is then rinsed with distilled water and dried. The film is then subjected to a series of treatments to remove any surface contaminants. This includes heating the film in a vacuum oven, followed by treatment with a solution of hydrogen peroxide and sulfuric acid. The final step is to rinse the film with distilled water and dry it. The resulting nickel film is then ready for use in adsorption studies.

## CHAPTER VI

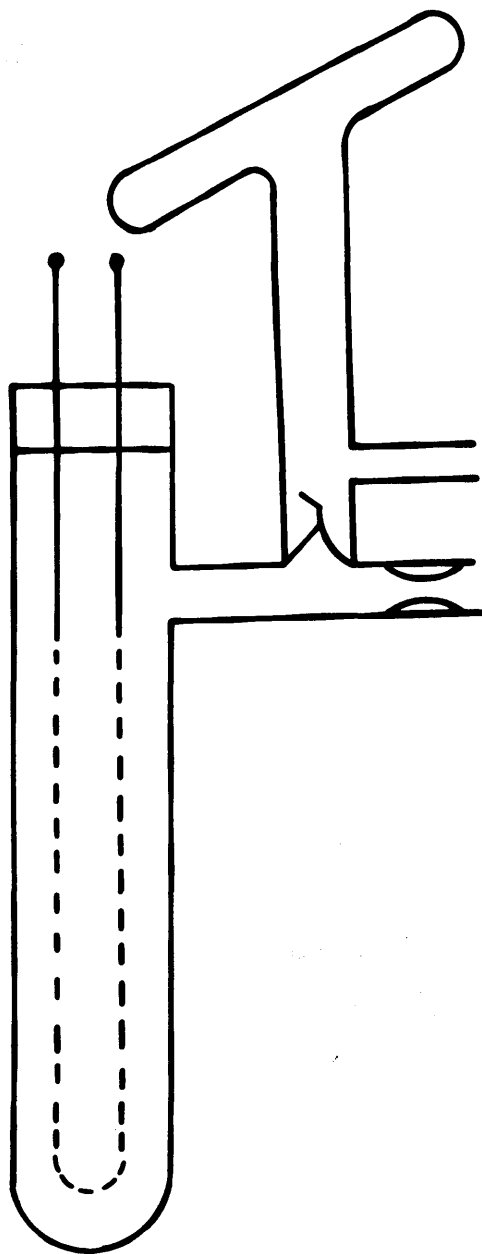
### Preparation of Nickel Films for Adsorption Studies

#### 6.1 Construction of Catalyst Vessel

Although various types of catalyst vessels were used these tended to differ only in minor details. The design of the simplest and most commonly used type is shown in fig. 18. The vessel consisted basically of a 2 cm. diameter Pyrex tube in which was suspended a nickel filament supported on tungsten leads. Messrs. Johnson Matthew supplied the 1 mm. diameter annealed tungsten wire used to make the tungsten leads. This wire was cut into 10 cm. lengths, heated to dull red heat and cleaned with sodium nitrite stick. This procedure was necessary to remove the surface coating of graphite. The reaction was rapid and exothermic, and care had to be taken to avoid appreciable loss of tungsten by reaction with the sodium nitrite. The leads were then washed with distilled water to remove any adhering sodium nitrite, heated in a gas air flame until an irridescent blue-green coating of tungsten oxide had been formed, and sleeved with 7 cm. lengths

**FIG.18**

**Catalyst vessel**



of Pyrex tubing. The sleeving, after degassing by heating to dull red heat, was melted on to the tungsten in an oxygen blow pipe flame, care being taken to avoid localised over heating. This resulted in a glass to metal seal of characteristic bronze colour. The filament was a 20 cm. length of pure nickel wire 0.02" diameter as supplied by Messrs. Johnson Matthey. The ends of the nickel filament were wound spirally around the tungsten leads and spot welded in order to make a good electrical contact. The prepared filament was bent into a hairpin shape and sealed into the Pyrex tube, 18 cm. long and 2 cm. in diameter, by making a pinch-seal on to the Pyrex covered tungsten leads. The side arm comprising the constriction and break-seal was joined to this tube below the glass to metal seal, and the whole annealed in a gas-air flame. The ends of the tungsten leads protruding from the catalyst vessel were completely covered with silver solder to seal the laminae against gas leakage. The filament was straightened and centred in the Pyrex tube, and the lower end of this tube closed and rounded off. The completed

vessels were then joined to the section of the apparatus designed for the preparation of the film.

In earlier designs of catalyst vessels the tungsten leads were much shorter and were consequently immersed in liquid nitrogen during surface area determinations. This arrangement was found to result in leakage at the tungsten leads.

Slightly different catalyst vessels were used for the experiments in which metallic caesium and radio-mercury were used as adsorbates. The construction of these catalyst vessels is discussed and shown in Chapter IV.

## 6.2 Treatment of Catalyst Vessel before film deposition

Before a nickel film free from surface contamination could be prepared, it was necessary to degas thoroughly the walls of the catalyst vessel and the nickel filament by heating under high vacuum conditions. Tubular furnaces were used for this purpose. These were wound, on a metal former 15 cm. long and 3 cm. diameter, with nichrome tape to a cold resistance

of 220 ohms. These furnaces attained a temperature of 500°C with an applied voltage of 240 volts. An iron-constantan thermocouple was used to monitor the temperature of the furnaces. These furnaces were placed round the catalyst vessels which were heated under high vacuum for a period of 24 hours.

During the last 12 hours of this treatment the filaments were degassed by raising their temperature gradually by means of an electric current to a temperature just below the evaporation temperature. This condition was achieved with a current of 4.2 amps. with the furnace at 500°C. Considerable gas evolution took place during the degassing process causing the pressure in the system to rise from  $10^{-5}$  mm. Hg to  $10^{-3}$  mm Hg. The filament was then flashed several times by passing a current of 6 amps. This was done to ensure complete degassing, since Anderson<sup>38</sup> has reported that nickel wire contains appreciable amounts of dissolved gases. The constriction was then degassed before sealing off the catalyst vessel. This was done by heating in it the yellow flame of a glass blowing torch until the flame became orange in colour, which

indicated that the glass had been heated to softening point. This was repeated several times to ensure complete degassing. The catalyst vessel was then sealed-off using the oxygen flame.

### 6.3 Deposition of Nickel Film

In order to prevent undue sintering of the nickel film during the deposition it was necessary to ensure that the walls of the vessel were kept cool. The vessels were immersed in a large beaker of water kept at room temperature. This system was chosen so that no further sintering of the film would occur while it was at room temperature between surface area determinations. The deposition of the film was effected by heating the films electrically.<sup>100</sup> Careful control of the heating current was required as high currents resulted in fusion and consequent breakage of the filament before sufficient nickel had been deposited, while low currents resulted in inconveniently slow evaporation rates.

Satisfactory results were obtained with a current of 6.5 amps. Evaporation rates of 30 to 40 mg. nickel

per hour were obtained under these conditions. At evaporation temperature the filament was almost at white heat. By this method films of weight 20 to 30 mg., mirror-like in appearance, were produced.

#### 6.4 Estimation of Nickel

The nickel films used in the adsorption measurements normally had a weight of 20 to 25 mg. and consequently gravimetric measurements were considered to be too insensitive for accurate determinations. Colorimetric methods were favoured as they afforded an accurate and straight forward method of determination. There are several methods available<sup>101</sup> which are based on the water soluble nickel III dimethylglyoxime complex.

The following solutions were prepared.

Nitric acid approximately 10N

Potassium bromate-bromide mixture

(3g  $\text{KBrO}_3$  and 12 g KBr per litre giving  
0.1N bromine on acidification)

Dimethylglyoxime solution

(1% in ethanol).

Ammonia solution

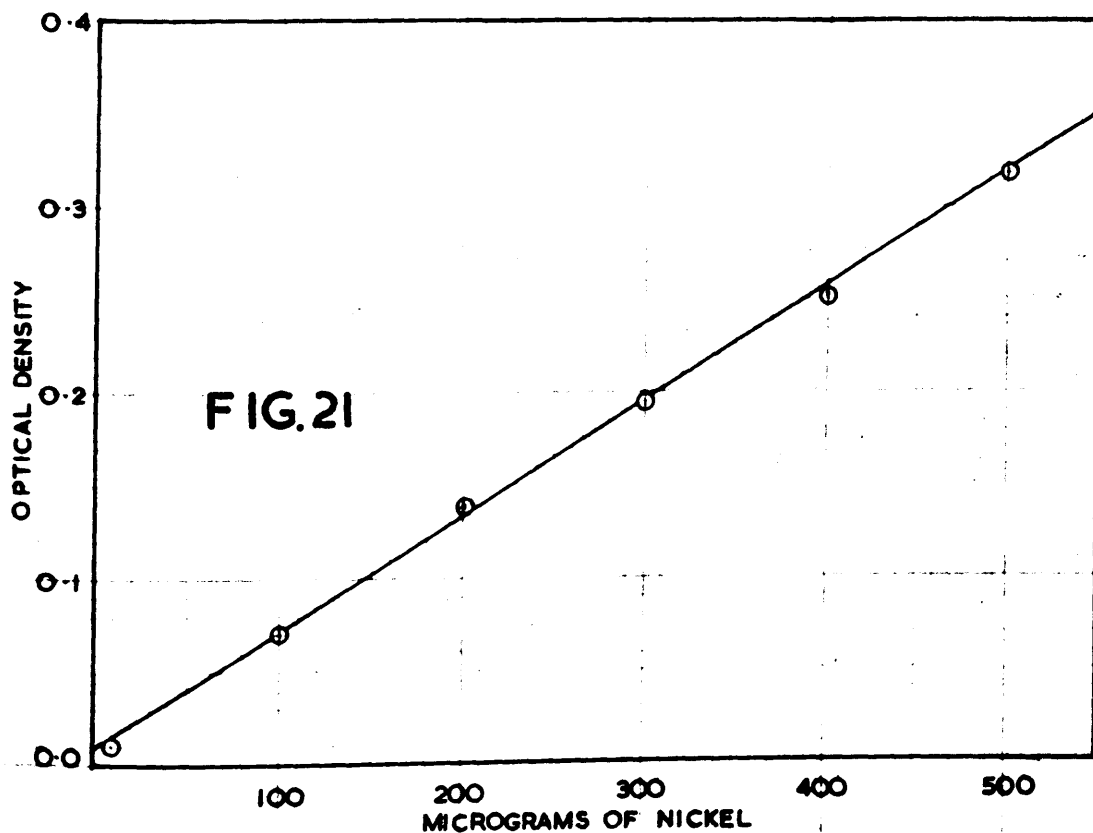
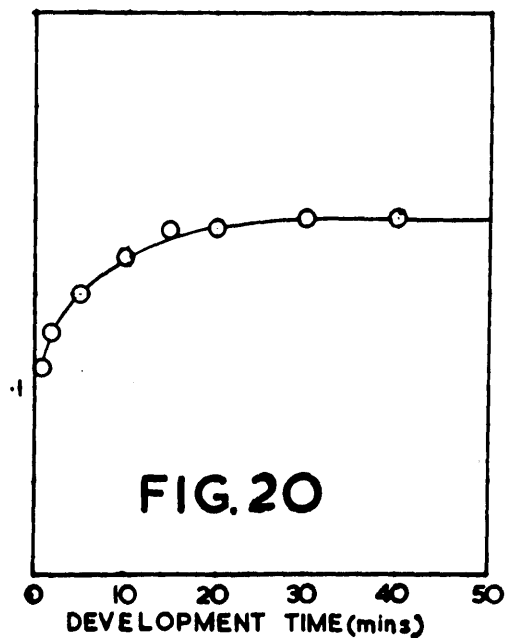
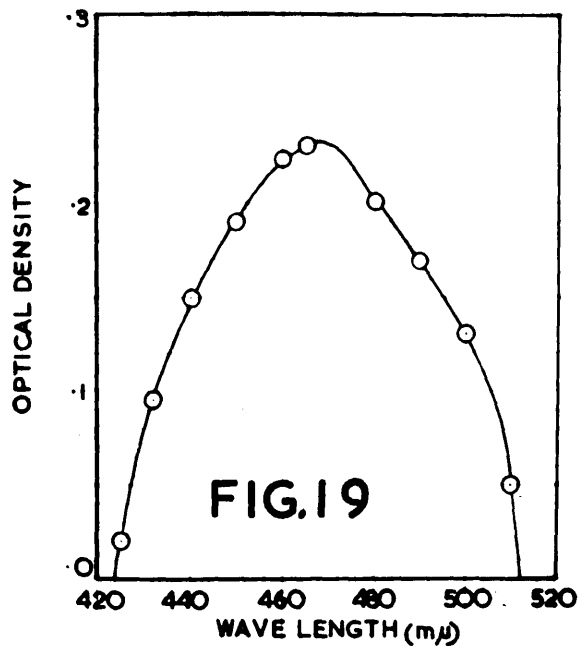
(0.88 ammonia diluted 1:10 with water)



The nickel film to be estimated was dissolved in 25 ml. of warm 10N nitric acid and the solution diluted to 1 litre with distilled water in a standard flask. 10 ml. of this solution was pipetted into a 50 ml. standard flask, and 10 ml. of the bromate-bromide mixture was added to oxidise the nickel II to the trivalent state, when the solution gradually became yellow due to the liberation of excess bromine. 1 ml. of dimethylglyoxime was then added followed by 10 ml. of ammonia solution. An orange red solution was produced which was diluted to 50 ml. with distilled water.

Previous tests<sup>102</sup> had been carried out to determine the absorption spectrum and the effect of time on the colour intensity of the complex. As shown in Fig. 19, the spectrum had an absorption peak at 465 m $\mu$  as measured on a Unicam SP 500 U.V. spectrophotometer. Fig. 20, shows that no further intensification of the colour occurs after 25 minutes, and readings were therefore taken after 30 minutes development. Measurements of the optical density of the solutions were made with the solution in a 1.0 cm. glass absorption cell at a wavelength of 465 m $\mu$ .

# COLORIMETRIC ESTIMATION OF NICKEL



Weighed lengths of the same pure nickel wire, used for the filaments, were dissolved in nitric acid in the same manner as a nickel film, in order to prepare a series of standard solutions containing about 10, 20, 30 and 40 mg. of nickel per litre of solution. From these standards a calibration curve shown in fig. 21, was constructed, but to ensure complete reproducibility of the method it was found more satisfactory to carry out the same complex formation procedure on 10 ml. samples of these standard solutions and to measure their optical density simultaneously with the unknown solution. The practise was to employ two standard nickel solutions, and to determine the weights of the unknown film by interpolation.

# APPENDIX A

Derivation of the expression used to calculate the volume of krypton adsorbed, and the pressure at which this adsorption took place.

Volume C = volume of catalyst vessel

Volume M = volume cut off McLeod gauge

Volume D = volume of connecting dead space.

All pressure readings were in mm. of mercury.

All volumes were in  $\text{cm}^3$ .

and all quantities were in  $\text{cm}^3$  mm.

A sample of krypton was admitted from the reservoir to volumes D and M. The McLeod gauge read  $a_1 b_1$  where  $a_1$  was the distance between the mercury in the closed limb and the top of the closed limb, and  $b_1$  was the difference in height between the mercury in the closed and open limb. The readings  $a_1$  and  $b_1$  were in cm.

$$\therefore \text{Quantity of gas in volumes D + M} = \frac{10Aa_1b_1(D + M)}{M} \text{ cm}^3 \text{ mm.}$$

where A = cross sectional area of the McLeod capillary  
in  $\text{cm}^2$ .

This quantity of gas was then allowed to expand into the catalyst vessel C, and the McLeod gauge then read  $a_2, b_2$ .

∴ Quantity in gas phase in volume D+M+C

$$= (D+M+C) \frac{10Aa_2b_2}{M}$$

∴ Quantity of gas adsorbed =  $\frac{10A}{M} [(D+M)a_1b_1 - (D+M+C)a_2b_2]$

$$= V_e \text{ cm}^3 \text{ mm.}$$

$$\text{Equilibrium pressure } P = \frac{10Aa_2b_2}{M} \text{ mm.}$$

Volume D was then evacuated, and the gas in volumes C and M allowed to expand into volume D. After equilibrium had been reached the McLeod gauge read  $a_3, b_3$ .

∴ Volume adsorbed =  $\frac{10A}{M} [(D+M)a_1b_1 - (D+M+C)a_3b_3 - Da_2b_2]$

$$\text{The new equilibrium pressure} = \frac{10Aa_3b_3}{M} \text{ mm.}$$

It follows that the general form of this expression is:

$$V_e = \frac{10A}{M} \left[ (D+M)a_1 b_1 - (D+M+C)anbn - \sum D_{an-1} b_{n-1} \right]$$

$$P = \frac{10Aanbn}{M}$$

The unit  $\frac{10A}{M} = \frac{10.\pi .r^2}{M}$  where  $r$  = radius of capillary tubing  
 $= 0.075$  cm.

$$= \frac{10.\pi .(0.075)^2}{137.90}$$

$$= 1.282 \times 10^{-3} \text{ cm}^{-1}$$

APPENDIX B

Calibration of McLeod gauge volume M

Weight of McLeod gauge + distilled water	=	260.685 gm.
Weight of McLeod gauge empty	=	122.510 gm.
∴ Weight of water filling gauge	=	138.175 gm.
Temperature of water	=	19°C
Density of water at 19°C	=	0.99843 gm. per ml.
∴ Corrected volume M	=	137.90 cm <sup>3</sup>

The smaller McLeod gauge, which was occasionally used to operate in a higher pressure range, was calibrated in a similar fashion. The corrected volume was found to be 34.53.cm<sup>3</sup>.

APPENDIX C

A Typical Surface Area Determination

The following surface area determination is for film No. 10 which appears in the results in table 3, Chapter II.

McLeod gauge readings for krypton adsorption on clean film

$H_1 - H_2$	a	$H_1' - H_2$	b
21.167 - 4.920	16.274	20.998 - 4.920	16.078
21.167 - 17.720	3.447	21.379 - 17.720	3.659
21.167 - 17.882	3.285	20.960 - 17.882	3.078
21.168 - 18.069	3.099	21.144 - 18.069	3.075
21.168 - 18.106	3.062	21.040 - 18.106	2.834
21.168 - 18.416	2.752	21.220 - 18.416	2.804
21.167 - 18.418	2.749	21.050 - 18.418	2.632
21.167 - 18.554	2.613	21.046 - 18.554	2.492
21.170 - 18.630	2.540	21.030 - 18.630	2.400
21.167 - 18.794	2.373	21.154 - 18.794	2.360
21.164 - 18.924	2.240	21.070 - 18.924	2.146

$H_1$  = Height of top of closed limb

$H_1'$  = Height of mercury level in open limb

$H_2$  = Height of mercury in closed limb

a =  $H_1 - H_2$

b =  $H_1' - H_2$



Using the expression derived in Appendix A the volume of krypton adsorbed and the pressure at which this adsorption took place was calculated as follows.

$$V_E = \frac{LOA}{M} \left[ (D+M)a_1 b_1 - (D+M+C)a_n b_n - \left[ D a_{n-1} b_{n-1} \right] \right]$$

$$P_E = \frac{LOA a_n b_n}{M}$$

$$\text{Volume } (D+M) = 214 \text{ cm}^3$$

$$\text{Volume } (D+M+C) = 448 \text{ cm}^3 = \text{apparent volume at } -195^\circ\text{C.}$$

$$\text{Volume } D = 76 \text{ cm}^3$$

$$V_E = 1.282 \times 10^{-3} \times 214 \times 16.247 \times 16.078 - 448 \times 3.447 \times 3.659$$

$$= 1.282 \times 10^{-3} \times 55,901 - 5650$$

$$= 64.4 \text{ cm}^3 \text{ mm.}$$

$$P_E = 1.282 \times 10^{-3} \times 3.447 \times 3.659 = 1.617 \times 10^{-2} \text{ mm.}$$

After the initial adsorption of krypton the dead space, volume D, was successively evacuated to give a series of readings. The calculation of these volumes of adsorbed krypton and the pressure of adsorption follows.

$$\begin{aligned}VE &= 1.282 \times 10^{-3} [214 \times 16.247 \times 16.078 - 448 \times 3.285 \times 3.078 - 76(3.447 \times 3.659)] \\&= 1.282 \times 10^{-3} [55,901 - 4,530 - 958] \\&= 64.6 \text{ cm}^3 \text{ mm}\end{aligned}$$

$$PE = 1.282 \times 10^{-3} \times 3.285 \times 3.078 = 1.300 \times 10^{-2} \text{ mm}.$$

$$\begin{aligned}VE &= 1.282 \times 10^{-3} [214 \times 16.247 \times 16.078 - 448 \times 3.099 \times 3.075 - 76(12.61 + 3.285 \times 3.078)] \\&= 1.282 \times 10^{-3} [55,901 - 4,269 - 1,727] \\&= 63.9 \text{ cm}^3 \text{ mm}\end{aligned}$$

$$PE = 1.282 \times 10^{-3} \times 3.099 \times 3.075 = 1.220 \times 10^{-2} \text{ mm}.$$

$$\begin{aligned}VE &= 1.282 \times 10^{-3} [214 \times 16.247 \times 16.078 - 448 \times 3.062 \times 3.075 - 76(22.72 + 3.099 \times 3.075)] \\&= 1.282 \times 10^{-3} [55,901 - 3,888 - 2,451] \\&= 63.5 \text{ cm}^3 \text{ mm}.\end{aligned}$$

$$PE = 1.282 \times 10^{-3} \times 3.062 \times 2.834 = 1.110 \times 10^{-3} \text{ mm}.$$

$$\begin{aligned}VE &= 1.282 \times 10^{-3} [214 \times 16.247 \times 16.078 - 448 \times 2.752 \times 2.804 - 76(32.25 + 3.062 \times 2.834)] \\&= 1.282 \times 10^{-3} [55,901 - 3,457 - 3,110] \\&= 63.2 \text{ cm}^3 \text{ mm}.\end{aligned}$$

$$PE = 1.282 \times 10^{-3} \times 2.752 \times 2.804 = 0.990 \times 10^{-2} \text{ mm}.$$

$$\begin{aligned} VE &= 1.282 \times 10^{-3} [214 \times 16.247 \times 16.078 - 448 \times 2.749 \times 2.632 - 76(40.92 + 2.752 \\ &\quad \times 2.804)] \\ &= 1.282 \times 10^{-3} [55,901 - 3,241 - 3,697] \\ &= 62.8 \text{ cm}^3 \text{ mm.} \end{aligned}$$

$$PE = 1.282 \times 10^{-3} \times 2.749 \times 2.632 = 0.927 \times 10^{-2} \text{ mm.}$$

$$\begin{aligned} VE &= 1.282 \times 10^{-3} [214 \times 16.247 \times 16.078 - 448 \times 2.613 \times 2.492 - 76(48.64 + 2.749 \\ &\quad \times 2.632)] \\ &= 1.282 \times 10^{-3} [55,901 - 2,917 - 4,247] \\ &= 62.5 \text{ cm}^3 \text{ mm.} \end{aligned}$$

$$PE = 1.282 \times 10^{-3} \times 2.61 \times 2.492 = 0.835 \times 10^{-2} \text{ mm.}$$

$$\begin{aligned} VE &= 1.282 \times 10^{-3} [214 \times 16.247 \times 16.078 - 448 \times 2.540 \times 2.400 - 76(55.88 + 2.613 \\ &\quad \times 2.492)] \\ &= 1.282 \times 10^{-3} [55,901 - 2,731 - 4,742] \\ &= 62.1 \text{ cm}^3 \text{ mm.} \end{aligned}$$

$$PE = 1.282 \times 10^{-3} \times 2.540 \times 2.400 = 0.782 \times 10^{-2} \text{ mm.}$$

$$\begin{aligned} VE &= 1.282 \times 10^{-3} [214 \times 16.247 \times 16.078 - 448 \times 2.373 \times 2.360 - 76(62.39 \times 2.540 \\ &\quad \times 2.400)] \\ &= 1.282 \times 10^{-3} [55,901 - 2,509 - 5,205] \\ &= 61.8 \text{ cm}^3 \text{ mm.} \end{aligned}$$

$$PE = 1.282 \times 10^{-3} \times 2.373 \times 2.360 = 0.618 \times 10^{-2} \text{ mm}$$

$$\begin{aligned} VE &= 1.282 \times 10^{-3} [214 \times 16.47 \times 16.078 - 448 \times 2.240 \times 2.146 - 76(68.49 + 2.373 \\ &\quad \times 2.360)] \\ &= 1.282 \times 10^{-3} [55,901 - 2,154 - 5,631] \\ &= 61.7 \text{ cm}^3 \text{ mm.} \end{aligned}$$

$$PE = 1.282 \times 10^{-3} \times 2.240 \times 2.146 = 0.616 \times 10^{-2} \text{ mm.}$$

$\frac{VE}{cm^3 mm.}$	$PE \times 10^{-2} mm.$	$P_o$ mm.	$\frac{PE}{P_o} \times 10^{-2}$	$\frac{PE}{VE P_o} \times 10^{-4}$
64.4	1.617	2.3	0.703	1.092
64.6	1.300	2.3	0.565	0.875
63.9	1.220	2.3	0.531	0.830
63.5	1.110	2.3	0.483	0.761
63.2	0.990	2.3	0.431	0.682
62.8	0.927	2.3	0.403	0.642
62.5	0.835	2.3	0.363	0.582
62.1	0.782	2.3	0.340	0.547
61.8	0.718	2.3	0.312	0.505
61.7	0.616	2.3	0.268	0.433

$P_o$  = saturated vapour pressure of krypton at the temperature of adsorption.

$\frac{PE}{P_o}$  was plotted against  $\frac{PE}{VE P_o}$  when a straight line resulted

of slope  $\frac{1}{V_m}$  which gave  $V_m = 67.2 \text{ cm}^3 \text{ mm.}$  (fig. 22)

FIG. 22

$$\frac{P_E}{V_E P_0} \times 10^{-5}$$

B.E.T. PLOT

FILM No. 10

1

2

3

4

5

6

7

8

9

10

11

1

2

3

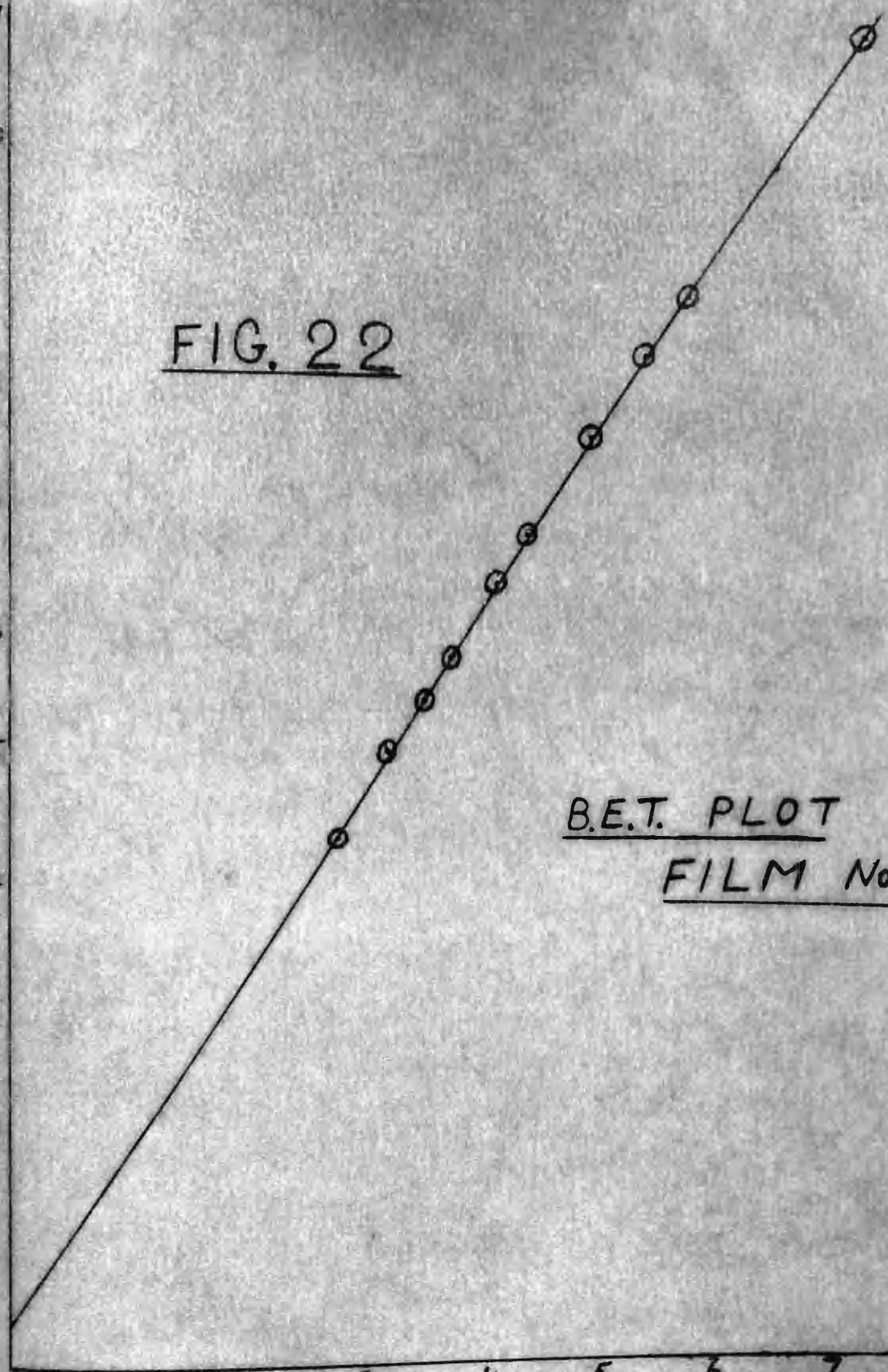
4

5

6

7

$$P_E/P_0 \times 10^{-3}$$



REFERENCES

1. Trapnell, B.M.W., Chemisorption p. 218  
Butterworths Scientific Publication.
2. Benton, A.F., J. Amer. Chem. Soc., 48, 1850 (1926).
3. Emmett, P.H. and Brunauer, S., J. Amer. Chem. Soc.,  
59, 310 (1937).
4. Emmett, P.H. and Brunauer, S., J. Amer. Chem. Soc.,  
59, 1553 (1937).
5. Beeck, O., Advances in Catalysis II p. 151  
New York Academic Press Inc., (1950).
6. Rideal, E.K. and Trapnell, B.M.W., Proc. Roy. Soc.,  
A205, 409 (1951)
7. de Boer, J.H. and Dippel, C.F., Z.Physik. Chem.,  
B3, 407 (1929).
8. de Boer, J.H., Rec. Trav. Chim., 65, 576 (1946)
9. Benton, A.F. and White, T.A., J. Amer. Chem. Soc.,  
54, 1820 (1932).
10. Brunauer, S., Emmett, P.H. and Teller, J. Amer. Chem.  
Soc., 59, 2682 (1937)
11. Brunauer, S. and Emmett, P.H. and Teller, E.J.  
J. Amer. Chem. Soc., 60, 309 (1938)

12. Klemperer, D.F. and Stone, F.S., Proc. Roy. Soc. A243, 375, (1957).
13. Roberts, W., Trans. Faraday Soc., 56, 128 (1960).
14. Bagg and Tompkins, Trans. Faraday Soc., 51, 1071 (1955).
15. Tunzi Okamoto, J. Physic. Soc., Japan, 2, 225 (1958).
16. Stone, F.S. and Tiley, P.F. Nature, 167, 654 (1951).
17. Tiley, P.F., Nature, 168, 434 (1951).
18. Cannon, P., J. Phys. Chem., 63, 1292 (1959).
19. Crawford, Roberts, W. and Kemball, Trans. Faraday Soc., 58, 1761 (1962).
20. Suhrman, R. and Schultz, K.2., Z. Physic. Chem. (Frankfurt) (N.F.), 1, 69, (1954).
21. Langmuir, I., J. Amer. Chem. Soc., 40, 1361 (1918).
22. Baly, E.C.C., Proc. Roy. Soc., A160, 465, (1937).
23. Brunauer, S., Emmett, P.H. and Teller, E.J., J. Amer. Chem. Soc., 59, 2682 (1937).
24. Brunauer, S., Emmett, P.H. and Teller, E.J., J. Amer. Chem. Soc., 59, 310, (1937).
25. Brunauer, S., Emmett, P.H. and Teller, E.J., J. Amer. Chem. Soc., 57, 1754 (1935).
26. Emmett, P.H., J. Amer. Chem. Soc., 68, 1784 (1946).

27. Koke, J. and Emmett, P.H., J. Amer. Chem. Soc., 80, 2082 (1958).
28. Beeck, O., Advances in Catalysis II p. 155 (1950).
29. Trapnell, B.M.W., Proc. Roy. Soc., A218, 566 (1953).
30. Pickering, H.L. and Eckstom, H.C., J. Amer. Chem. Soc., 74, 4775 (1952).
31. Johansen, R.T., Lorenz, P.B., Dodd, C.G., Pidgeon, F.D., and Davies, J.W., J. Phys. Chem., 57, 40, (1953).
32. Davies, R.T., DeWitt, T.N., and Emmett, P.H., J. Phys. Chem., 51, 1232 (1947).
33. Wolock, I. and Harris, B.L., Indust. Engng. Chem., 42, 1347 (1950)
34. Beeck, O. and Ritchie, A.W., Disc. Faraday Soc., 8, 159 (1950).
35. Zettlemoyer, A.C., Chand, A. and Gamble E.J., J. Amer. Chem. Soc., 72, 2752 (1950).
36. Cosgrave, L.A., J. Phys. Chem., 51, 664, (1947).
37. Hall, R.A.W. and Swart, E.R., Z. Elektrochem., 61, 380 (1957).
38. Anderson, J.R. and Baker, B.G., J. Phys. Chem., 66, 482, (1962).
39. Ehrlich, G. and Hudda, F.G., J. Chem. Phys., 30, 493, (1959).



40. Gaines, G.L. and Cannon, P., J. Phys., Chem.,  
64, 997, (1960)
41. Roberts, M.W., Nature, 182, 1151, 1205 (1958)
42. Roberts, M.W., Trans. Faraday Soc., 56, 128 (1960)
43. Trapnell, B.M.W., "Chemisorption", p.3. Butterworths  
Scientific Publications.
44. Kingston, G.L. and Holmes, J.M., Trans. Faraday Soc.,  
49, 417, (1953)
45. See Handbook of Chemistry and Physics, 36th Edn.,  
p. 2157. Chemical Rubber Publishing Co., Cleveland,  
Ohio.
46. Tominago and Keii, T., Anal. Chem., 1965, (1961)
47. See Keii, T., "Surface Chemistry" Volume 7, "Experimental  
Chemistry" Japanese Chemical Society.
48. Innes, W.B., Anal. Chem., 23, 759 (1951)
49. Orr, C., (Jr) and Dallavalle, J.M. "Fine Particle  
Measurement" p. 183, MacMillan, New York (1959)
50. Knudsen, Ann. Physik., 31, 205 (1910).
51. Porter, A.S., Disc. Faraday Soc., 8, 358 (1950).
52. Rosenberg, A.J. J. Amer. Chem. Soc., 78, 2929 (1956).
53. Rosenberg, A.J. and Martel, C.S., J. Phys. Chem.,  
62, 457, (1958)
54. Loss, J.M. and Fergusson, R.R., Trans. Faraday Soc.,  
48, 730 (1952).

55. Liang, S.C., J. Phys. Chem., 57, 910 (1953)
56. Liang, S.C. J. Appl. Phys., 22, 148 (1951)
57. Liang, S.C., J. Phys. Chem., 56, 660 (1952).
58. Liang, S.C., Canad. J. Chem., 33, 279 (1955)
59. Klemperer, and Stone, F., Proc. Roy. Soc., A243, **375 (1957)**
60. Brennan, Hayward and Trapnell, B.M.W., Proc. Roy. Soc., A256, 81 (1960).
61. Jeck, Actes du Deuxieme International de Catalyse (Paris, 1960), 2, 2285.
62. Anderson, Phys. Chem. Solids, 16, 291 (1960)
63. Zettlemoyer, A.C., Yu, Y.F., Chessick, J.J. and Hesley, F.H., J. Phys. Chem., 61, 1319 (1957).
64. Pritchard, J., Nature, 194, 38 (1962).
65. Mignolet, J.C.P., Disc. Faraday Soc., 8, 108, (1950).
66. Culver, R.V. and Tompkins, .C., Advances in Catalysis 11, 67 (1959).
67. Ponec and Knor, Collection, Czech. Chem. Commun., 27, 1091 (1962).
68. Cassie, A.B.D., Trans. Faraday Soc., 41, 450, (1945).
69. Hill, T.L., J. Chem. Phys. 14, 263 (1946).
70. Hill, T.L., J. Chem. Phys., 16, 181 (1948).
71. Kemball, C. and Schreiner, G.D.L., J. Amer. Chem. Soc., 72, 5605 (1950)

72. Kemball, C. and Rideal, E.K., Proc. Roy. Soc.,  
A187, 53 (1946).
73. Cassel, H. and Neugelbrauer, W., J. Phys. Chem., 40,  
523, (1936).
74. Kemball, C., Advances in Catalysis 2, 240 (1949).
75. Gregg, S.J. and Jacobs, J., Trans. Faraday Soc.,  
44, 574 (1948)
76. Pritchard, J. Trans. Faraday Soc., 59, 1963, (437).
77. See Mignolet, J.C.P., "Chemisorption" p. 18. Edited  
by Garner, W.E., Butterworths Scientific Publications  
(1957).
78. Ogawa, I., Doke, T. and Nakada, I. J. Appl. Phys.  
(Japan) 21, 223, (1952).
79. Bosworth, R.C.L., Trans. Faraday Soc., 35, 397 (1939).
80. Beebe, R.A., Beckwith, J.B. and Honig, J.M. J. Amer.  
Soc., 67, ~~1554~~ (1945)
81. Pickering, H.L. and Eckstrons, H.C., J. Amer. Chem.  
Soc., 74, 4775 (1952).
82. Johansen, R.T., Lorenz, P.B., Dodd, C.G., Pidgeon,  
F.D. and Davies, J.W. J. Phys. Chem. 57, 40 (1953).
83. Haul, R.A.W. Agnew, Chem. 68, 238 (1956).
84. Davies, R.T. DeWitt, T.W. and Emmett, P.H.,  
J. Phys. Chem. 51, 1232 (1947).

85. Zettlemoyer, A.C. Chand. A. and Gamble, E.,  
J. Amer. Chem. Soc., 72, 2752 (1950).
86. Singleton and Halsey, J. Phys. Chem. 58, 330 (1954).
87. Campbell, K.C. and Thomson, S.J., Trans. Faraday Soc.,  
55, 985 (1959).
88. See Wells, A.F. Structural Inorganic Chemistry, 2nd.  
Edn. p. 689, Oxford Clarendon Press.
89. Langmuir, I. and Taylor, J.B., Phys. Rev., 40,  
463 (1932).
90. Langmuir, I. and Taylor, J.B., Phys. Rev., 44,  
423 (1933).
91. See, Leck, "Pressure Measurement in Vacuum Systems",  
London, The Institute of Physics, 264, (1957).
92. Porter, Trans. Faraday Soc., 29, 702 (1932).
93. Rosenberg, Res. Sci. Instr., 10, 258 (1938)
94. Klemperer, J. Sci. Instr., 21, 88 (1944)
95. Haase, Z. Tech. Physik., 24, 27 (1943)
96. See Dudkman, Vacuum Technique, Chapman and Hall, Ltd.,  
London, 12 (1955).
97. Rosenberg. Rev. Sci. Instr., 10, 131 (1939).
98. Cranstoun, G.K.L., Ph.D. Thesis, Glasgow 177 (1962)
99. See Partington, J.R. "An advanced Treatise on Physical  
Chemistry". p.924

100. Campbell, K.C., Ph.D. Thesis, Durham, 144 (1958).
101. See Vogel, "A Text Book of Quantitative Inorganic Analysis," Longmans Green and Co., London, 654 (1951).
102. Campbell, K.C., Ph.D. Thesis, Durham, (1958).